

## Function space requirements for the single-electron functions within the multiparticle Schrödinger equation

Martin J. Mohlenkamp

Citation: *J. Math. Phys.* **54**, 062105 (2013); doi: 10.1063/1.4811396

View online: <http://dx.doi.org/10.1063/1.4811396>

View Table of Contents: <http://jmp.aip.org/resource/1/JMAPAQ/v54/i6>

Published by the [AIP Publishing LLC](#).

---

### Additional information on J. Math. Phys.

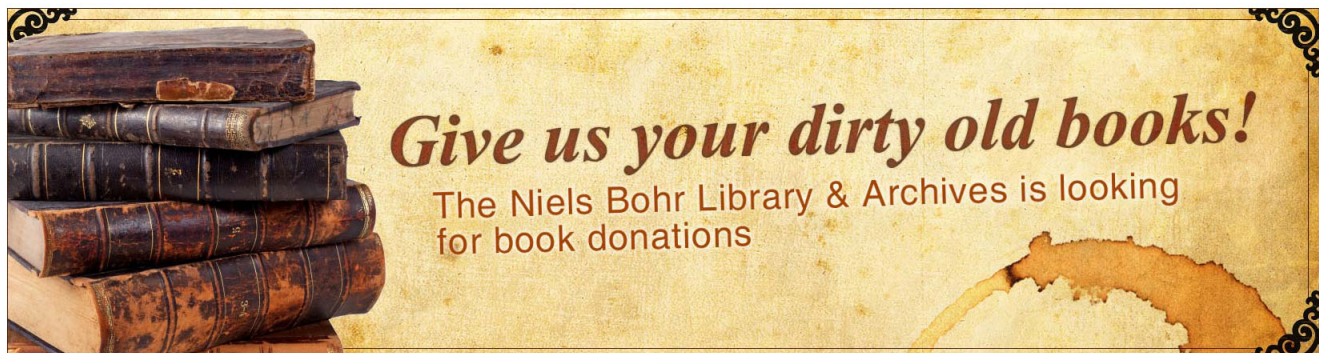
Journal Homepage: <http://jmp.aip.org/>

Journal Information: [http://jmp.aip.org/about/about\\_the\\_journal](http://jmp.aip.org/about/about_the_journal)

Top downloads: [http://jmp.aip.org/features/most\\_downloaded](http://jmp.aip.org/features/most_downloaded)

Information for Authors: <http://jmp.aip.org/authors>

### ADVERTISEMENT



*Give us your dirty old books!*

The Niels Bohr Library & Archives is looking  
for book donations

# Function space requirements for the single-electron functions within the multiparticle Schrödinger equation

Martin J. Mohlenkamp<sup>a)</sup>

*Department of Mathematics, Ohio University, Athens, Ohio 45701, USA*

(Received 11 September 2012; accepted 4 June 2013; published online 24 June 2013)

Our previously described method to approximate the many-electron wavefunction in the multiparticle Schrödinger equation reduces this problem to operations on many single-electron functions. In this work, we analyze these operations to determine which function spaces are appropriate for various intermediate functions in order to bound the output. This knowledge then allows us to choose the function spaces in which to control the error of a numerical method for single-electron functions. We find that an efficient choice is to maintain the single-electron functions in  $L^2 \cap L^4$ , the product of these functions in  $L^1 \cap L^2$ , the Poisson kernel applied to the product in  $L^4$ , a function times the Poisson kernel applied to the product in  $L^2$ , and the nuclear potential times a function in  $L^{4/3}$ . Due to the integral operator formulation, we do not require differentiability. © 2013 AIP Publishing LLC. [<http://dx.doi.org/10.1063/1.4811396>]

## I. INTRODUCTION

We consider the time-independent, non-relativistic,  $N$ -electron multiparticle Schrödinger equation with the Born-Oppenheimer approximation that the nuclei are point charges. This equation is an eigenproblem  $\mathcal{H}\psi = \lambda\psi$ . The eigenvalues  $\lambda$  correspond to energies and the smallest energies are of greatest interest. The wavefunction  $\psi$  is a function of  $N$  variables, each of which has a three-dimensional spatial part  $\mathbf{r} = (x, y, z)$  and a spin variable  $\sigma \in \{-1/2, 1/2\}$ , which we combine as  $\gamma = (\mathbf{r}, \sigma)$ . The wavefunction  $\psi$  is also required to be antisymmetric under the exchange of any two  $\gamma_i$  and  $\gamma_j$  for  $i \neq j$ , a constraint that can be written as  $\mathcal{A}\psi = \psi$  where  $\mathcal{A}$  is the orthogonal projector onto the space of antisymmetric functions. The Hamiltonian  $\mathcal{H} = \mathcal{T} + \mathcal{V} + \mathcal{W}$  consists of kinetic, nuclear potential, and inter-electron potential operators defined, respectively, by

$$\mathcal{T} = -\frac{1}{2} \sum_{i=1}^N \nabla_i^2, \quad \mathcal{V} = \sum_{i=1}^N V(\mathbf{r}_i), \quad \text{and} \quad \mathcal{W} = \frac{1}{2} \sum_{i=1}^N \sum_{j \neq i}^N \frac{1}{\|\mathbf{r}_i - \mathbf{r}_j\|}. \quad (1)$$

The differential operator  $\nabla^2$  is a three-dimensional Laplacian, and the potential  $V(\mathbf{r})$  is a sum of terms of the form  $-Z_a/\|\mathbf{r} - \mathbf{r}_a\|$  from a nucleus of charge  $0 < Z_a$  at position  $\mathbf{r}_a$ .

Following the paradigm of separated representations,<sup>1,2</sup> in Ref. 3 we developed methods to compute approximate wavefunctions of the form

$$\psi_{(R)}(\gamma_1, \gamma_2, \dots, \gamma_N) = \mathcal{A} \sum_{l=1}^R \prod_{i=1}^N \phi_i^l(\gamma_i), \quad (2)$$

where the number of terms  $R$  controls the quality of the approximation. The novelty introduced in Ref. 3 is that the single-electron functions  $\phi_i^l$  in (2) are unconstrained: they need not come from some basis set, follow some excitation pattern, or satisfy orthogonality conditions. Even without constraints, the representation (2) shares certain well-known flaws with the configuration interaction method. To alleviate these flaws, we extended the methods of Ref. 3 to scale properly for large

<sup>a)</sup>Electronic mail: [mohlenka@ohio.edu](mailto:mohlenka@ohio.edu). URL: [www.ohio.edu/people/mohlenka/](http://www.ohio.edu/people/mohlenka/).

systems<sup>4</sup> and to capture the inter-electron cusp.<sup>5</sup> See the introduction to Ref. 5 for an extended discussion of the motivation for this approach and comparison with other approaches. Briefly, the advantage of this approach is that it may allow very efficient expansions and an unbiased exploration of the structure of the wavefunction. The first disadvantage of this approach is that conceptual novelties in it require new mathematics and algorithms to be developed. In Refs. 4 and 5 we filled in some of the required pieces, and in the current work we fill in another piece. The second disadvantage is that it might fail. Specifically, the gains from having very efficient representations may not be worth the trouble of finding them. Resolving this issue requires the completion of the mathematical and algorithm development and then numerical comparisons with existing methods.

In Sec. IA, we sketch the algorithm from Ref. 3. The algorithm reduces to a sequence of operations on functions of a single electron coordinate  $\gamma$ . In Sec. IB, we introduce the main subject of this paper, which is the analysis of these operations on the single-electron functions with the goal of determining which function spaces are appropriate for various intermediate functions in order to bound the output. The analysis is surprisingly, and at times unpleasantly, rich.

### A. Sketch of the algorithm

We give only a skeletal sketch of the algorithm, and in particular refer the reader to Ref. 3 for a proper discussion of the origins and attribution of the component ideas. The algorithm starts with an initial estimate  $\mu \approx \lambda$  and initial  $\{\phi_i^l\}_{i,l}$  and then proceeds as follows:

**Loop 1:** until  $\mu$  converges.

**Copy:**  $\{\phi_i^l\}_{i,l}$  to  $\{\tilde{\phi}_i^l\}_{i,l}$ .

**Loop 2:** until  $\{\phi_i^l\}_{i,l}$  converges.

**Copy:**  $\{\tilde{\phi}_i^l\}_{i,l}$  to  $\{\phi_i^l\}_{i,l}$  and normalize.

**Loop 3:** until  $\{\tilde{\phi}_i^l\}_{i,l}$  converges.

**Loop 4:**  $k = 1, \dots, N$ .

**Update:**  $\{\tilde{\phi}_k^l\}_l$  using  $\mu$ ,  $\{\phi_i^l\}_{i,l}$ , and  $\{\tilde{\phi}_i^l\}_{i,l}$ .

**Update:**  $\mu$  using  $\{\phi_i^l\}_{i,l}$  and  $\{\tilde{\phi}_i^l\}_{i,l}$ .

The update of  $\mu$  in Loop 1 uses  $\psi$  formed from  $\{\phi_i^l\}_{i,l}$  via (2) and  $\tilde{\psi}$  formed from  $\{\tilde{\phi}_i^l\}_{i,l}$  via (2), which correspond to the previous and newest approximate wavefunctions produced in Loop 2. In Sec. IIB, we (re)derive and justify the update rule

$$\mu \leftarrow \mu - \frac{\langle (\psi - \tilde{\psi}), (\mathcal{V} + \mathcal{W})\psi \rangle}{\|\tilde{\psi}\|^2}. \quad (3)$$

To a product  $\prod_{i=1}^N \phi_i(\gamma_i)$  we associate a column vector of  $N$  functions of a single variable,

$$\Phi = [\phi_1, \phi_2, \dots, \phi_N]^*, \quad (4)$$

where  $(\cdot)^*$  denotes (conjugate) transpose; we also use  $\Phi$  as shorthand for the product itself. The antisymmetric inner product of two such products is computed by (Löwdin's rule)

$$\langle \mathcal{A}\tilde{\Phi}, \mathcal{A}\Phi \rangle = \langle \mathcal{A}\tilde{\Phi}, \Phi \rangle = \frac{1}{N!} |\mathbb{L}| \quad (5)$$

using the matrix  $\mathbb{L}$  with entries

$$L(i, j) = \langle \tilde{\phi}_i, \phi_j \rangle. \quad (6)$$

To compute antisymmetric inner products involving  $\mathcal{V}$  or  $\mathcal{W}$ , first compute  $\mathbb{L}$  from (6), then construct  $\Theta = \mathbb{L}^{-1} \tilde{\Phi}$ , and then use the formulas

$$\langle \mathcal{A}\tilde{\Phi}, \mathcal{V}\Phi \rangle = \frac{|\mathbb{L}|}{N!} \int \mathcal{V} \Phi^* \Theta d\gamma \quad \text{and} \quad (7)$$

$$\langle \mathcal{A}\tilde{\Phi}, \mathcal{W}\Phi \rangle = \frac{1}{2} \frac{|\mathbb{L}|}{N!} \int \Phi^* \Theta \mathcal{W}_p [\Phi^* \Theta] + \Phi^* \mathcal{W}_p [\Theta \Phi^*] \Theta d\gamma, \quad (8)$$

where

$$\mathcal{W}_{\mathcal{P}}[f](\mathbf{r}) = \int \frac{1}{\|\mathbf{r} - \mathbf{r}'\|} f(\gamma') d\gamma' = \sum_{\sigma' \in \{-1/2, 1/2\}} \int \frac{1}{\|\mathbf{r} - \mathbf{r}'\|} f(\mathbf{r}', \sigma') d\mathbf{r}'. \quad (9)$$

We can thus compute the update of  $\mu$  (3) by linear combinations of computations using (5), (7), and (8).

Loop 2 is a Green function iteration. For  $\mu < 0$ , define the Green function

$$\mathcal{G}_{\mu} = (\mathcal{T} - \mu\mathcal{I})^{-1}. \quad (10)$$

The differential eigenvalue problem  $\mathcal{H}\psi = (\mathcal{T} + \mathcal{V} + \mathcal{W})\psi = \lambda\psi$  corresponds to the integral equation  $-\mathcal{G}_{\lambda}(\mathcal{V} + \mathcal{W})\psi = \psi$ . Given an estimate  $\mu \approx \lambda$  for the lowest eigenvalue, one can perform a power iteration

$$\tilde{\psi} \leftarrow -\mathcal{G}_{\mu}[(\mathcal{V} + \mathcal{W})\psi] \quad \text{and} \quad (11)$$

$$\psi \leftarrow \tilde{\psi} / \|\tilde{\psi}\| \quad (12)$$

to produce an approximate eigenfunction. Note that (11) preserves the antisymmetry constraint  $\psi = \mathcal{A}\psi$ .

Loops 3 and 4 are an iterative least-squares fitting. To maintain the representation (2) with  $R$  fixed we replace (11) with the definition that  $\tilde{\psi}$  is the function of the form (2) that minimizes the error

$$\|\tilde{\psi} - (-\mathcal{G}_{\mu}[(\mathcal{V} + \mathcal{W})\psi])\|. \quad (13)$$

Loop 3 controls the overall convergence of  $\tilde{\psi}$  and Loop 4 varies which functions  $\{\tilde{\phi}_k^l\}_l$  we optimize over.

The innermost update of  $\{\tilde{\phi}_k^l\}_l$  is a linear least-squares problem, which can be solved by solving a linear system  $\mathbb{A}\mathbf{x} = \mathbf{b}$  (the normal equations). For  $k = 1$ , the matrix  $\mathbb{A}$  consists of integral operators defined by

$$A(l, l')(\gamma, \gamma') = \left\langle \mathcal{A}\delta(\gamma - \gamma_1) \prod_{i=2}^N \tilde{\phi}_i^l(\gamma_i), \delta(\gamma' - \gamma_1) \prod_{i=2}^N \tilde{\phi}_i^{l'}(\gamma_i) \right\rangle \quad (14)$$

and the vector  $\mathbf{b}$  consists of functions defined by

$$b(l)(\gamma) = \sum_{m=1}^R \left\langle \mathcal{A}\delta(\gamma - \gamma_1) \prod_{i=2}^N \tilde{\phi}_i^l(\gamma_i), -\mathcal{G}_{\mu}[\mathcal{V} + \mathcal{W}] \prod_{i=1}^N \phi_i^m(\gamma_i) \right\rangle. \quad (15)$$

The entries of  $\mathbb{A}$  in (14) are computed by modifying (5) to account for the delta functions. Defining  $\mathbf{w}(\gamma') = [\tilde{\phi}_2^l(\gamma') \dots \tilde{\phi}_N^l(\gamma')]^*$ ,  $\mathbf{y}(\gamma) = [\tilde{\phi}_2^{l'}(\gamma) \dots \tilde{\phi}_N^{l'}(\gamma)]^*$ , and

$$\mathbb{D} = \begin{bmatrix} \langle \tilde{\phi}_2^l, \tilde{\phi}_2^{l'} \rangle & \dots & \langle \tilde{\phi}_2^l, \tilde{\phi}_N^{l'} \rangle \\ \vdots & \ddots & \vdots \\ \langle \tilde{\phi}_N^l, \tilde{\phi}_2^{l'} \rangle & \dots & \langle \tilde{\phi}_N^l, \tilde{\phi}_N^{l'} \rangle \end{bmatrix}, \quad (16)$$

we have

$$A(l, l')(\gamma, \gamma') = \frac{|\mathbb{D}|}{N!} (\delta(\gamma - \gamma') - \mathbf{y}^*(\gamma) \mathbb{D}^{-1} \mathbf{w}(\gamma')). \quad (17)$$

To compute  $\mathbf{b}$ , we first approximate the Green function as a sum of Gaussian convolution operators. Since Gaussians are separable, we obtain a separated representation

$$\mathcal{G}_{\mu} \approx \sum_{j=1}^J \bigotimes_{i=1}^N \mathcal{F}_{\mathbf{r}_i}^j, \quad (18)$$

where the subscript  $\mathbf{r}_i$  indicates in which variable the operator is applied, the superscript  $j$  indicates which operator to apply, and the dependence on  $\mu$  is implicit. We then have

$$b(l)(\gamma) \approx - \sum_{m=1}^R \sum_{j=1}^J \left\langle \mathcal{A} \mathcal{F}_{\mathbf{r}_1}^j \delta(\gamma - \gamma_1) \prod_{i=2}^N \mathcal{F}_{\mathbf{r}_i}^j \tilde{\phi}_i^l(\gamma_i), [\mathcal{V} + \mathcal{W}] \prod_{i=1}^N \phi_i^m(\gamma_i) \right\rangle. \quad (19)$$

For fixed indexes  $l, m$ , and  $j$ , all the terms in (19) are of the form

$$\left\langle \mathcal{A} \mathcal{F}_{\mathbf{r}_1} \delta(\gamma - \gamma_1) \prod_{i=2}^N \mathcal{F}_{\mathbf{r}_i} \tilde{\phi}_i(\gamma_i), [\mathcal{V} + \mathcal{W}] \prod_{i=1}^N \phi_i(\gamma_i) \right\rangle. \quad (20)$$

To evaluate them, we modify the formulas (7) and (8) to account for the presence of  $\mathcal{F}$  and  $\delta(\gamma - \gamma_1)$ . First, construct the matrix of inner products  $\mathbb{L}$  (6) but using  $\mathcal{F}\tilde{\phi}_i$  in place of  $\tilde{\phi}_i$ . Then construct a vector  $\mathbf{d}$  that is orthogonal to all but the first row of  $\mathbb{L}$  and has norm one. Let  $\mathbb{E}$  be the matrix  $\mathbb{L}$  with the first row replaced by  $\mathbf{d}^*$  and let  $\Theta = \mathbb{E}^{-1} \mathcal{F} \tilde{\Phi}$ . Then (20) is computed by

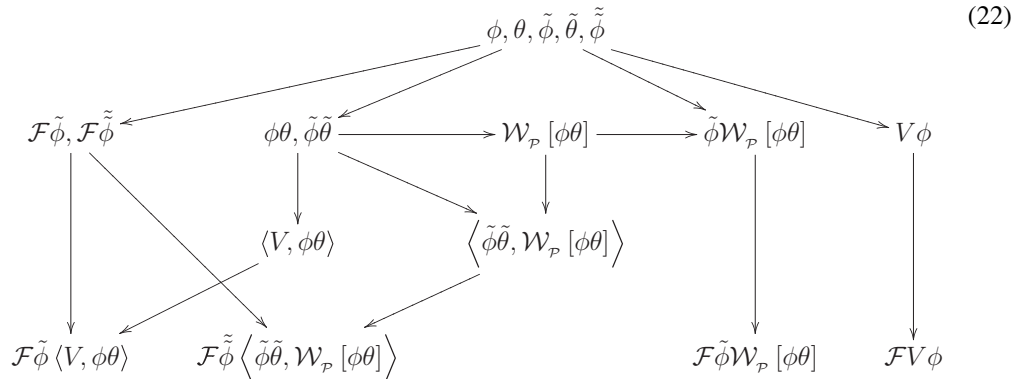
$$\begin{aligned} & \frac{|\mathbb{E}|}{N!} \mathcal{F} \left[ \Phi^* \mathbf{d} \int V \Phi^* \Theta d\gamma' - \Phi^* \int V \Phi^* \mathbf{d} \Theta d\gamma' + \frac{1}{2} \Phi^* \mathbf{d} \int \Phi^* \Theta \mathcal{W}_{\mathcal{P}} [\Phi^* \Theta] d\gamma' \right. \\ & - \frac{1}{2} \Phi^* \mathbf{d} \int \Phi^* \mathcal{W}_{\mathcal{P}} [\Theta \Phi^*] \Theta d\gamma' - \Phi^* \int \Theta \mathcal{W}_{\mathcal{P}} [\Phi^* \Theta] \Phi^* \mathbf{d} d\gamma' - \Phi^* \int \Theta \Phi^* \mathcal{W}_{\mathcal{P}} [\Theta \Phi^* \mathbf{d}] d\gamma' \\ & \left. + V \Phi^* \mathbf{d} + \Phi^* \mathbf{d} \mathcal{W}_{\mathcal{P}} [\Phi^* \Theta] - \Phi^* \mathcal{W}_{\mathcal{P}} [\Theta \Phi^* \mathbf{d}] \right] (\gamma). \quad (21) \end{aligned}$$

In this formula, the integrands are all functions or vectors of functions of the suppressed variable  $\gamma'$ , so after integration they yield scalars or column vectors. Applying  $\Phi^*$  or  $\Phi^* \mathbf{d}$  on the left yields a function. In the last row, where there are no integrals, we directly obtain a function. Applying  $\mathcal{F}$  to the sum of all these functions yields a single function of  $\gamma$ .

The algorithm is thus performed using only linear combinations of computations of the forms (5), (7), (8), (17), and (21) which only use operations on the single-electron functions  $\{\phi_i^l\}_{i,l}$  and  $\{\tilde{\phi}_i^l\}_{i,l}$ . Thus the algorithm reduces the  $N$ -electron problem to operations on the single-electron functions. The operations required are:

- product of functions;
- inner product of functions;
- multiplication of a function by the nuclear potential  $V$ ;
- application of  $\mathcal{W}_{\mathcal{P}}[\cdot]$ , which is convolution with the Poisson kernel  $1/\|\mathbf{r}\|$ ; and
- application of operators  $\mathcal{F}$ , which are convolutions with Gaussians.

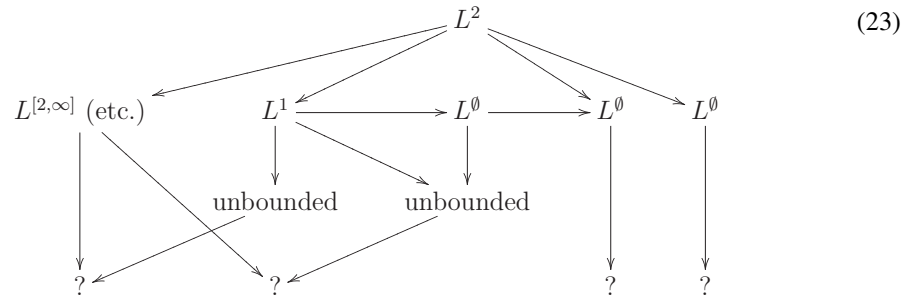
The operations used in (5), (7), (8), and (17) are a subset of those needed for (21) so we restrict our discussion to (21). The operations in (21) are performed according to the diagram



where  $\phi, \theta, \tilde{\phi}, \tilde{\theta}, \tilde{\tilde{\phi}}$  are single-electron functions. Note that (22) does not include any projections onto a basis set, but instead asks for accurate representations of functions.

## B. Operations on single-electron functions

The numerical method used for the operations in (22) is independent of Ref. 3, and hence in Refs. 3, 4, and 5 we did not address it, or provide overall numerical results. In principle a suitable numerical method was demonstrated in Refs. 6 and 7, but when we tried to use it as implemented in Ref. 8 there were unacceptable losses of accuracy. With hindsight the cause is clear: Controlling the error of  $\phi_i^l$  in  $L^2$  does not bound the error of the results of the operations in (22). If we assume only that  $\phi_i^l \in L^2$  and track the function spaces to which the objects in (22) belong, we obtain



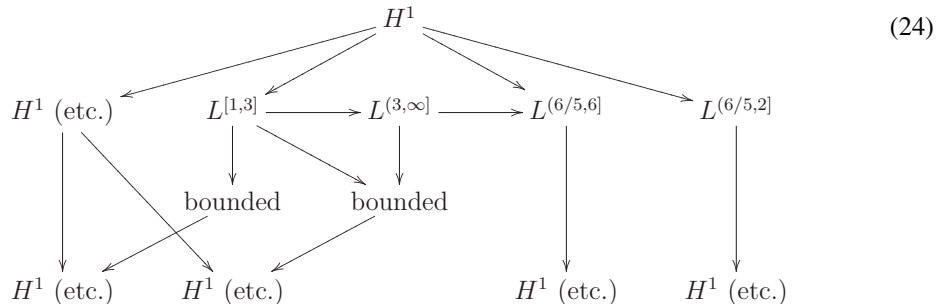
where  $L^\emptyset$  indicates that the function is not in any  $L^p$  space and  $L^{[2,\infty]}$  indicates that it is in  $L^p$  for  $2 \leq p \leq \infty$ . Since the outputs of (22) will be used in an iteration, they should have the same properties as the inputs, but in (23) they do not. The functions  $\phi_i^l$  are actually in much nicer function spaces than  $L^2$ , both from general theoretical considerations<sup>9</sup> and because the operator  $\mathcal{F}$  that produced them in the previous iteration is very nice. The problem is that the difference between  $\phi_i^l$  and its numerical approximation is only known to be in  $L^2$ , and this error propagates according to (23). For example, if  $\phi$  is some nice function and we approximate it with  $f$  such that  $\|\phi - f\|_2 < \epsilon$ , then the error  $\|V(\phi - f)\|_p$  can be infinite.

The goals of the current paper are:

1. Determine function spaces so that the operations in (22) produce bounded errors.
2. From among those function space options that produce bounded errors, select those that will be most efficient to implement.
3. Provide bounds and benchmark problems that can be used to test numerical methods to see if they are good enough to use for (22).

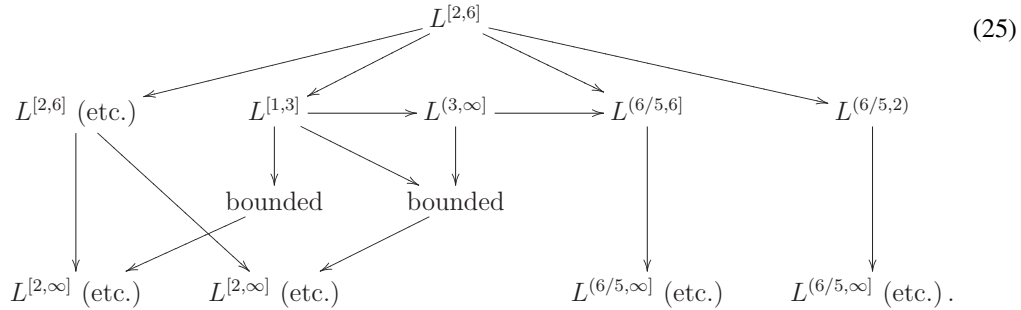
As a preliminary step, in Sec. II C, we analyze the Green function and its approximation (19) so that we can reduce our analysis to a single Gaussian convolution  $\mathcal{F}$  rather than a collection of them. We also note that the presence of the spin coordinate  $\sigma$  introduces at worst a small constant in the bounds, so we replace the combined variable  $\gamma$  with the physical variable  $\mathbf{r}$  for our further analysis.

The natural function space in which to consider  $\phi_i^l$  is the Sobolev space  $H^1(\mathbf{R}^3)$ , since that is the smallest space in which the energy computation is meaningful when  $N = 1$ . When we assume  $\phi_i^l \in H^1$ , then the function space diagram becomes



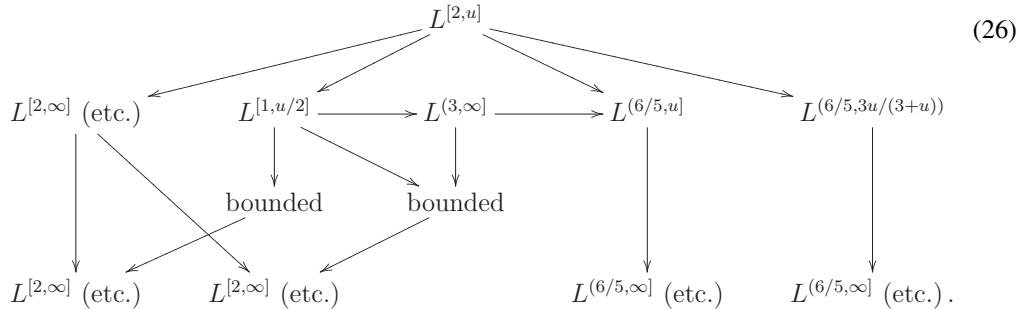
and the diagram completes successfully, with bounded errors.

On the other hand, we use an integral operator formulation of the problem, so none of our operations involve differentiation. Although one cannot directly compute the energy without (at least weak) differentiation, one can infer the energy from the integral equation. In Sec. II B, we derive such an energy estimate. The Sobolev embedding theorem says  $H^1(\mathbf{R}^3) \subset L^6(\mathbf{R}^3)$ , so we have  $H^1 \subset L^{[2,6]}$ . We therefore consider  $L^{[2,6]}$  as our candidate for a space that does not use derivatives but is only slightly weaker than  $H^1$ . If we replace  $H^1$  with  $L^{[2,6]}$ , then the function space diagram becomes



Since  $L^{(6/5,\infty]} \subset L^{[2,\infty]} \subset L^{[2,6]}$  these operations successfully return us to our original space. The only substantial change from (24) is that we no longer have  $V\phi \in L^2$ .

Having boldly discarded differentiability, we can then consider weakening our function spaces further. All else being equal, weaker function spaces place weaker requirements on the numerical method, and thus should allow easier/faster codes. We can weaken  $L^{[2,6]}$  by considering  $L^{[2,u]}$  for some  $u < 6$ . (We require  $L^2$  for basic inner products, so we do not consider weakening at the  $L^2$  end.) We find that  $3 < u$  allows successful completion of the diagram, but at  $u = 3$  the scalar  $|\langle V, \phi\theta \rangle|$  becomes unbounded. Under the assumption  $3 < u$ , the function space diagram becomes



In Sec. III, we present our main analysis of these function space diagrams. First, we demonstrate the divergence of (23). Then we prove (26), which contains (25) as a corollary, and then enhance (25) to obtain (24).

The above analysis indicates what we *can* do, but is not sufficient to determine what we *should* do. From among the allowed options, we need to specify in which norms the numerical algorithm should control the errors in which objects. We restrict ourselves to combinations of  $L^p$ -spaces based on (26). We do not argue specifically against  $H^1$ , mainly because we have found no good way to compare against it. We also wish to allow methods that use discontinuous basis functions<sup>6–8</sup> and so cannot control  $H^1$  error. For similar reasons, we do not consider Besov spaces or other spaces. To make these decisions we consider three primary factors:

1. A weaker function space is preferred since it is easier for the numerical method to accomplish.
2. Spaces should be chosen to allow the singularities in the operators to be truncated at as large a radius as possible.
3. Spaces should be chosen to give the best bounds on the final outputs.

The analysis is complicated by the fact that multiple norms are in use and several of the operations are nonlinear. Without further information, we cannot make our decisions. We therefore consider a test case, the “core orbital,” which is the exact solution for one electron on one atom.

We use the core orbital to select parameters in the operators and to test the bounds. In Sec. IV, we introduce the core orbital and use it to analyze the influence of the choice of spaces on the bounds and truncation radii. Based on our analysis we recommend that the spaces be chosen as

$$\begin{array}{c}
 L^2 \cap L^4 \\
 \swarrow \quad \searrow \quad \searrow \quad \searrow \\
 L^2 \cap L^4 \quad L^1 \cap L^2 \quad L^4 \quad L^2 \quad L^{4/3} \\
 \downarrow \quad \downarrow \quad \downarrow \quad \downarrow \quad \downarrow \\
 L^2 \cap L^4 \quad (\text{scalar}) \quad (\text{scalar}) \quad L^2 \cap L^4 \quad L^2 \cap L^4 \\
 \downarrow \quad \downarrow \quad \downarrow \quad \downarrow \quad \downarrow \\
 L^2 \cap L^4 \quad L^2 \cap L^4 \quad L^2 \cap L^4 \quad L^2 \cap L^4 \quad L^2 \cap L^4
 \end{array} \tag{27}$$

The choice of  $\mathcal{W}_p[\phi\theta] \in L^4$  is the result of balancing larger truncation radius for  $L^p$  with smaller  $p$  against bounds exploding due to the constraint  $3 < p$ . The choice of  $V\phi \in L^{4/3}$  balances the truncation radii for  $V\phi$  and  $\mathcal{F}$ .

In Sec. V, we gather information useful for implementing and testing numerical methods trying to perform the operations in (22) while controlling the error in the spaces in (27). First, we collect bounds from throughout the paper and insert the parameters in (27) to provide a complete list of the bounds used for (27). Next we collect the truncation radii allowed for the cusps and singularities using the parameters in (27). Then we account for linear combinations present in (21) but neglected in (22). Then we present formulas for accurately computing antisymmetric inner products when the matrices involved are ill-conditioned. Finally, we provide a list of benchmark problems to use for validation and performance testing the method.

In this paper we prove that to perform the iteration in Ref. 3 it is sufficient for the numerical method for the single-electron functions to do the operations in (22) while controlling the error in the spaces in (27), we argue that (27) is an efficient choice, and we provide information to aid the implementation and testing of such a method. Development of enhancements to the numerical methods in Refs. 6–8 to satisfy our requirements is in progress and will be reported elsewhere.

## II. PRELIMINARY ANALYSIS

In this section, we first collect some background information, then discuss estimating the energy in the integral formulation, and then analyze the convolutions in the Green function to reduce our analysis to the operations in (22).

### A. Function space basics

(See, e.g., Ref. 10.) For a function on some domain  $\Omega$ , its  $L^p$  norm for  $1 \leq p < \infty$  is defined by

$$\|f\|_p = \left( \int_{\Omega} |f(t)|^p dt \right)^{1/p}, \tag{28}$$

and its  $L^\infty$  norm is defined by

$$\|f\|_\infty = \text{ess.sup.}_{t \in \Omega} |f(t)|, \tag{29}$$

which for continuous functions is equivalent to

$$\|f\|_\infty = \max_{t \in \Omega} |f(t)|. \tag{30}$$

Those functions with finite  $\|f\|_p$  are said to lie in  $L^p(\Omega)$ . The  $L^2$  inner product is defined by

$$\langle f, g \rangle = \int_{\Omega} f(t)g(t) dt \tag{31}$$

(for real functions). Hölder's inequality states

$$|\langle f, g \rangle| \leq \|f\|_p \|g\|_q \quad \text{for} \quad \frac{1}{p} + \frac{1}{q} = 1 \quad \text{with} \quad 1 \leq p, q \leq \infty. \quad (32)$$

For functions on a domain such that  $t \in \Omega$  and  $t' \in \Omega$  implies  $t - t' \in \Omega$ , convolution is defined by

$$(f * g)(t) = \int_{\Omega} f(t - t') g(t') dt'. \quad (33)$$

The Sobolev space  $H^1(\mathbf{R}^d) = W^{1,2}(\mathbf{R}^d)$  consists of functions with finite value for the norm

$$\|f\|_{H^1} = \left( \int |\hat{f}(\xi)|^2 + \sum_{i=1}^d |\xi_i \hat{f}(\xi)|^2 d\xi \right)^{1/2}, \quad (34)$$

where  $\hat{f}$  is the Fourier transform of  $f$  and  $\xi = (\xi_1, \dots, \xi_d)$ . We can write the norm as

$$\|f\|_{H^1} = (\|f\|_2^2 + \|\nabla f\|_2^2)^{1/2}, \quad (35)$$

with the implicit understanding that the gradient may only exist weakly. For our analysis we will separate the  $H^1$  norm into  $L^2$  norm and the  $L^2$  norm of the (weak) gradient, denoted  $L^2_{\nabla}$ .

## B. Energy estimate and update

Our goal is to solve the eigenproblem  $\mathcal{H}\psi = \lambda\psi$  for the minimal  $\lambda$  with the constraint  $\mathcal{A}\psi = \psi$ . The iteration (11) and (12) only provides an approximate  $\psi$ , so we still need a method to estimate  $\lambda$ . The step (11) uses  $\mu \approx \lambda$ , so the quality of  $\psi$  is limited by the quality of  $\mu \approx \lambda$ . Thus we also need a method to update and improve  $\mu$ .

For  $\psi$  satisfying  $\mathcal{H}\psi = \lambda\psi$  and  $\mathcal{A}\psi = \psi$ , the eigenvalue  $\lambda$  is the energy. The energy for any  $\psi = \mathcal{A}\psi$  is defined by the Rayleigh quotient

$$\frac{\langle \psi, \mathcal{H}\psi \rangle}{\|\psi\|^2}. \quad (36)$$

The expression (36) is variational, which provides two useful properties. First, the difference between this energy and  $\lambda$  is quadratic in the difference between  $\psi$  and the eigenfunction. Second, the energy produced by (36) is bounded below by  $\lambda$ , and so (36) provides an upper bound on  $\lambda$ . The numerator in (36) is computed using (7), (8), and

$$\langle \mathcal{A}\tilde{\Phi}, \mathcal{T}\Phi \rangle = \frac{1}{2} \frac{|\mathbb{L}|}{N!} \int (-\nabla^2 \Phi^*) \Theta d\gamma. \quad (37)$$

In order to compute (37), we need

$$\int \theta(\mathbf{r}) (-\nabla^2 \phi)^*(\mathbf{r}) d\gamma = \langle \theta, -\nabla^2 \phi \rangle = \langle \nabla \theta, \nabla \phi \rangle \quad (38)$$

to make sense and be finite. The minimal condition to assure this is  $\phi, \theta \in H^1$ . We can then bound by

$$|\langle \nabla \theta, \nabla \phi \rangle| \leq \|\nabla \theta\|_2 \|\nabla \phi\|_2. \quad (39)$$

To avoid requiring  $H^1$ , we wish to have an energy estimate that only uses integral quantities. Let us assume that the iteration (11) and (12) has converged, so that we have found an eigenfunction  $\psi_{\mu}$  and eigenvalue  $\alpha_{\mu}$  of the Lippmann-Schwinger integral equation

$$-\mathcal{G}_{\mu}(\mathcal{V} + \mathcal{W})\psi_{\mu} = \alpha_{\mu}\psi_{\mu}. \quad (40)$$

Inserting  $\psi_\mu$  into (36) and using (40), we obtain

$$\begin{aligned} \frac{\langle \psi_\mu, \mathcal{H} \psi_\mu \rangle}{\|\psi_\mu\|^2} &= \frac{\langle \psi_\mu, [\mu \mathcal{I} + (\mathcal{T} - \mu \mathcal{I}) + (\mathcal{V} + \mathcal{W})] \psi_\mu \rangle}{\|\psi_\mu\|^2} \\ &= \mu + \frac{\langle \psi_\mu, (\mathcal{T} - \mu \mathcal{I})(-1/\alpha_\mu) \mathcal{G}_\mu (\mathcal{V} + \mathcal{W}) \psi_\mu \rangle + \langle \psi_\mu, (\mathcal{V} + \mathcal{W}) \psi_\mu \rangle}{\|\psi_\mu\|^2} \\ &= \mu - \left( \frac{1 - \alpha_\mu}{\alpha_\mu} \right) \frac{\langle \psi_\mu, (\mathcal{V} + \mathcal{W}) \psi_\mu \rangle}{\|\psi_\mu\|^2}. \end{aligned} \quad (41)$$

If (40) is solved exactly, then (41) retains the variational properties of (36).

Now we observe from (40) and (41) that  $\psi_\mu$  is an eigenfunction of  $\mathcal{H}$  with eigenvalue  $\mu$  if and only if  $\alpha_\mu = 1$ . Defining  $f(\mu) = \alpha_\mu - 1$ , we can apply a step of Newton's method to obtain the update rule  $\mu \leftarrow \mu - f(\mu)/f'(\mu)$ . (The following argument to compute  $f'(\mu) = d\alpha_\mu/d\mu$  is due to Gregory Beylkin.) Applying  $\mathcal{G}_\mu^{-1/2}$  to both sides of (40) and rearranging, we obtain the related normalized eigenvalue equation

$$-\mathcal{G}_\mu^{1/2}(\mathcal{V} + \mathcal{W})\mathcal{G}_\mu^{1/2} \frac{\mathcal{G}_\mu^{-1/2} \psi_\mu}{\|\mathcal{G}_\mu^{-1/2} \psi_\mu\|} = \alpha_\mu \frac{\mathcal{G}_\mu^{-1/2} \psi_\mu}{\|\mathcal{G}_\mu^{-1/2} \psi_\mu\|}, \quad (42)$$

which has the form  $\mathcal{L}_\mu g_\mu = \alpha_\mu g_\mu$  with  $\mathcal{L}_\mu$  self-adjoint and  $\langle g_\mu, g_\mu \rangle = 1$ . Taking the inner product of both sides of (42) with  $g_\mu$  and solving for  $\alpha_\mu$ , we obtain  $\alpha_\mu = \langle \mathcal{L}_\mu g_\mu, g_\mu \rangle$ . Differentiating with respect to  $\mu$  and using (42) we obtain

$$\begin{aligned} \frac{d\alpha_\mu}{d\mu} &= \left\langle \frac{d\mathcal{L}_\mu}{d\mu} g_\mu, g_\mu \right\rangle + \left\langle \mathcal{L}_\mu \frac{dg_\mu}{d\mu}, g_\mu \right\rangle + \left\langle \mathcal{L}_\mu g_\mu, \frac{dg_\mu}{d\mu} \right\rangle \\ &= \left\langle \frac{d\mathcal{L}_\mu}{d\mu} g_\mu, g_\mu \right\rangle + \left\langle \frac{dg_\mu}{d\mu}, \mathcal{L}_\mu g_\mu \right\rangle + \left\langle \mathcal{L}_\mu g_\mu, \frac{dg_\mu}{d\mu} \right\rangle \\ &= \left\langle \frac{d\mathcal{L}_\mu}{d\mu} g_\mu, g_\mu \right\rangle + \alpha_\mu \frac{d}{d\mu} \langle g_\mu, g_\mu \rangle = \left\langle \frac{d\mathcal{L}_\mu}{d\mu} g_\mu, g_\mu \right\rangle. \end{aligned} \quad (43)$$

Using the explicit form  $\mathcal{G}_\mu^{1/2} = (\mathcal{T} - \mu \mathcal{I})^{-1/2}$  we can compute  $d\mathcal{G}_\mu^{1/2}/d\mu = \mathcal{G}_\mu^{3/2}/2$  and so

$$\frac{d\mathcal{L}_\mu}{d\mu} = -\frac{1}{2} \mathcal{G}_\mu^{3/2} (\mathcal{V} + \mathcal{W}) \mathcal{G}_\mu^{1/2} - \frac{1}{2} \mathcal{G}_\mu^{1/2} (\mathcal{V} + \mathcal{W}) \mathcal{G}_\mu^{3/2}. \quad (44)$$

Inserting into (43) and manipulating, we obtain

$$\begin{aligned} \frac{d\alpha_\mu}{d\mu} &= \left\langle \left[ -\frac{1}{2} \mathcal{G}_\mu^{3/2} (\mathcal{V} + \mathcal{W}) \mathcal{G}_\mu^{1/2} - \frac{1}{2} \mathcal{G}_\mu^{1/2} (\mathcal{V} + \mathcal{W}) \mathcal{G}_\mu^{3/2} \right] \frac{\mathcal{G}_\mu^{-1/2} \psi_\mu}{\|\mathcal{G}_\mu^{-1/2} \psi_\mu\|}, \frac{\mathcal{G}_\mu^{-1/2} \psi_\mu}{\|\mathcal{G}_\mu^{-1/2} \psi_\mu\|} \right\rangle \\ &= \frac{1}{2} \frac{\langle [-\mathcal{G}_\mu (\mathcal{V} + \mathcal{W}) - (\mathcal{V} + \mathcal{W}) \mathcal{G}_\mu] \psi_\mu, \psi_\mu \rangle}{\langle \mathcal{G}_\mu^{-1/2} \psi_\mu, \mathcal{G}_\mu^{-1/2} \psi_\mu \rangle} \\ &= \frac{1}{2} \frac{\langle -\mathcal{G}_\mu (\mathcal{V} + \mathcal{W}) \psi_\mu, \psi_\mu \rangle + \langle \psi_\mu, -\mathcal{G}_\mu (\mathcal{V} + \mathcal{W}) \psi_\mu \rangle}{\langle \mathcal{G}_\mu^{-1} \psi_\mu, \psi_\mu \rangle} \\ &= \frac{1}{2} \frac{2\alpha_\mu \langle \psi_\mu, \psi_\mu \rangle}{\langle \mathcal{G}_\mu^{-1} (-\alpha_\mu)^{-1} \mathcal{G}_\mu (\mathcal{V} + \mathcal{W}) \psi_\mu, \psi_\mu \rangle} = -\alpha_\mu^2 \frac{\langle \psi_\mu, \psi_\mu \rangle}{\langle (\mathcal{V} + \mathcal{W}) \psi_\mu, \psi_\mu \rangle}. \end{aligned} \quad (45)$$

Thus Newton's method yields the update rule

$$\mu \leftarrow \mu - \frac{f(\mu)}{f'(\mu)} = \mu - \left( \frac{1 - \alpha_\mu}{\alpha_\mu^2} \right) \frac{\langle \psi_\mu, (\mathcal{V} + \mathcal{W}) \psi_\mu \rangle}{\|\psi_\mu\|^2}. \quad (46)$$

We do not expect (40) to be solved exactly since we may not wait for (11) and (12) to converge, and in any case we make an error in our approximation (13). Thus we need to modify (41) and (46)

to use  $\psi$  and  $\tilde{\psi} = -\mathcal{G}_\mu(\mathcal{V} + \mathcal{W})\psi$  as in (11). We propose to use

$$\mu - \frac{\langle(\psi - \tilde{\psi}), (\mathcal{V} + \mathcal{W})\psi\rangle}{\langle\psi, \tilde{\psi}\rangle} \quad \text{and} \quad (47)$$

$$\mu \leftarrow \mu - \frac{\langle(\psi - \tilde{\psi}), (\mathcal{V} + \mathcal{W})\psi\rangle}{\|\tilde{\psi}\|^2}, \quad (48)$$

which reduce to (41) and (46) when  $\psi_\mu$  is inserted. The update rule (48) was given in Ref. 7 with the following derivation. Assume  $\psi$  is the true wavefunction, but  $\mu \neq \lambda$ . Then we have

$$\psi = -\mathcal{G}_\lambda(\mathcal{V} + \mathcal{W})\psi = -\mathcal{G}_\mu(\mathcal{V} + \mathcal{W})\psi - (\lambda - \mu)\mathcal{G}_\mu^2(\mathcal{V} + \mathcal{W})\psi + \mathcal{O}((\lambda - \mu)^2). \quad (49)$$

Neglecting the second-order term, taking the inner product with  $(\mathcal{V} + \mathcal{W})\psi$ , and rearranging, we obtain

$$\begin{aligned} \langle\psi, (\mathcal{V} + \mathcal{W})\psi\rangle &\approx \langle-\mathcal{G}_\mu(\mathcal{V} + \mathcal{W})\psi, (\mathcal{V} + \mathcal{W})\psi\rangle + \langle-(\lambda - \mu)\mathcal{G}_\mu^2(\mathcal{V} + \mathcal{W})\psi, (\mathcal{V} + \mathcal{W})\psi\rangle \\ \Rightarrow \langle\psi, (\mathcal{V} + \mathcal{W})\psi\rangle &\approx \langle\tilde{\psi}, (\mathcal{V} + \mathcal{W})\psi\rangle - (\lambda - \mu)\langle-\mathcal{G}_\mu\tilde{\psi}, (\mathcal{V} + \mathcal{W})\psi\rangle \\ \Rightarrow (\lambda - \mu)\langle\tilde{\psi}, \tilde{\psi}\rangle &\approx \langle\tilde{\psi} - \psi, (\mathcal{V} + \mathcal{W})\psi\rangle. \end{aligned} \quad (50)$$

Solving for  $\lambda$  yields (48).

### C. Analysis of the Gaussian convolutions in the Green function

In this section, we determine the effect of the Green function and its component convolutions.

#### 1. Convolution and Gaussians

For convolutions (33), Young's inequality states

$$\|f * g\|_s \leq \|f\|_p \|g\|_q \quad \text{for} \quad \frac{1}{p} + \frac{1}{q} = \frac{1}{s} + 1 \quad \text{with} \quad 1 \leq p, q, s \leq \infty. \quad (51)$$

Under the assumption that  $f$  is continuously differentiable and all the integrals converge

$$\nabla(f * g) = \nabla_{\mathbf{r}} \left( \int f(\mathbf{r} - \mathbf{r}') g(\mathbf{r}') d\mathbf{r}' \right) = \int (\nabla_{\mathbf{r}} f(\mathbf{r} - \mathbf{r}')) g(\mathbf{r}') d\mathbf{r}' = (\nabla f) * g. \quad (52)$$

The Fourier transform of a Gaussian in dimension  $d$  (see, e.g., Ref. 11) is

$$\int \exp(-\pi \tau \|\mathbf{r}\|^2) \exp(-2\pi i \langle \xi, \mathbf{r} \rangle) d\mathbf{r} = \tau^{-d/2} \exp(-\pi \|\xi\|^2 / \tau), \quad (53)$$

where  $\xi$  is also a  $d$ -dimensional variable. The special case  $\xi = 0$  provides

$$\int \exp(-\pi \tau \|\mathbf{r}\|^2) d\mathbf{r} = \tau^{-d/2} \quad (54)$$

and consequently

$$\|\exp(-\pi \tau \|\mathbf{r}\|^2)\|_p = \left( \int \exp(-\pi p \tau \|\mathbf{r}\|^2) d\mathbf{r} \right)^{1/p} = (p\tau)^{-d/(2p)}. \quad (55)$$

The integral representation for the Gamma function in Refs. 12 and 17 (Eq. (5.9.1)) provides the integral

$$\frac{\Gamma(\nu)}{z^\nu} = \int_0^\infty \exp(-zs) s^{\nu-1} ds \quad \text{for} \quad 0 < z \quad \text{and} \quad 0 < \nu. \quad (56)$$

Setting  $z = 1$  serves as a definition for the Gamma function. Using this integral identity we can also compute explicitly in  $d = 3$  that

$$\begin{aligned} \left\| \nabla e^{-\alpha \|\mathbf{r}\|^2} \right\|_p &= \left\| \left( \nabla e^{-\alpha \|\mathbf{r}\|^2} \cdot \nabla e^{-\alpha \|\mathbf{r}\|^2} \right)^{1/2} \right\|_p = \left\| -2\alpha \|\mathbf{r}\| e^{-\alpha \|\mathbf{r}\|^2} \right\|_p \\ &= \left( 4\pi (2\alpha)^p \int_0^\infty e^{-\alpha p r^2} r^{p+2} dr \right)^{1/p} = \left( 2\pi (2\alpha)^p \int_0^\infty e^{-\alpha p t} t^{(p+1)/2} dt \right)^{1/p} \\ &= \alpha^{-(p+1)/(2p)} 2 (2\pi \Gamma((p+3)/2) p^{-(p+3)/2})^{1/p}. \end{aligned} \quad (57)$$

## 2. Integral representation of the Green function

The Green function  $\mathcal{G}_\mu = (\mathcal{T} - \mu \mathcal{I})^{-1}$  in (10) is a convolution operator and thus is defined by its kernel. The Fourier transform of the kernel is given explicitly by

$$\hat{G}_\mu(\mathbf{z}) = \frac{1}{2\pi^2 \|\mathbf{z}\|^2 - \mu}, \quad (58)$$

where  $\mathbf{z} \in \mathbf{R}^{3N}$ . Setting  $v = 1$  in (56) and using the change of variables  $s = e^t$  we obtain

$$\frac{1}{z} = \int_{-\infty}^{\infty} \exp(-ze^t + t) dt. \quad (59)$$

Substituting  $z = (2\pi^2 \|\mathbf{z}\|^2 - \mu)/(-\mu)$  and then dividing by  $-\mu$  gives

$$\hat{G}_\mu(\mathbf{z}) = \int_{-\infty}^{\infty} \frac{\exp(-e^t + t)}{-\mu} \exp\left(-\frac{2\pi^2 e^t}{-\mu} \|\mathbf{z}\|^2\right) dt. \quad (60)$$

Applying the  $3N$ -dimensional inverse Fourier transform yields

$$\mathcal{G}_\mu = \int_{-\infty}^{\infty} \bigotimes_{i=1}^N \mathcal{F}_{\mathbf{r}_i}(t) dt, \quad (61)$$

where  $\mathcal{F}_{\mathbf{r}_i}(t)$ , which depends implicitly on  $\mu$ , is the operator that convolves with the Gaussian

$$F(t) = \left( \frac{\exp(-e^t + t)}{-\mu} \right)^{1/N} \left( \frac{-\mu}{2\pi e^t} \right)^{3/2} \exp\left(-\frac{\mu}{2e^t} \|\mathbf{r}\|^2\right) \quad (62)$$

in the variable  $\mathbf{r}_i$ . By discretizing (61) we will obtain an approximation for  $\mathcal{G}_\mu$  as a sum of separable convolutions with Gaussians. For our analysis of norms in Sec. II C 3 we will keep the integral form and then in Sec. II C 4 consider how to discretize it.

## 3. Operator norms

We now consider the operator  $\mathcal{F}(t)$  defined by convolution with the Gaussian (62). Using Young's inequality (51), the operator norm of  $\mathcal{F}(t) : L^q \rightarrow L^s$  for any  $1 \leq q \leq s$  is bounded by the  $L^p$  norm of the kernel of  $\mathcal{F}(t)$  with  $p = (1 + 1/s - 1/q)^{-1}$ . We can compute directly via (55) the  $L^p$  norm of the kernel (62) as

$$\|F(t)\|_p = \left( \frac{\exp(-e^t + t)}{-\mu} \right)^{1/N} \left( \frac{-\mu}{2\pi e^t} \right)^{3/2} \left( \frac{-\mu p}{2\pi e^t} \right)^{-3/(2p)}. \quad (63)$$

Since this is finite for all  $1 \leq p$ , we conclude that  $\mathcal{F}(t) : L^q \rightarrow L^s$  is bounded for any  $1 \leq q \leq s$ . Equivalently,  $f \in L^q$  implies  $\mathcal{F}(t)f \in L^{[q, \infty]}$ . We now consider how to bound  $\mathcal{F}(t) : L^q \rightarrow L^s_\nabla$  for  $1 \leq q \leq s$ . Using (52) and Young's inequality (51), our bound is the  $L^p$  norm of the kernel of  $\nabla \mathcal{F}(t)$

with  $p = (1 + 1/s - 1/q)^{-1}$ . We can compute using (57) that

$$\|\nabla F(t)\|_p = \left( \frac{\exp(-e^t + t)}{-\mu} \right)^{1/N} \left( \frac{-\mu}{2\pi e^t} \right)^{3/2} \left( \frac{-\mu}{2e^t} \right)^{-(p+1)/(2p)} 2 \left( \Gamma \left( \frac{p+3}{2} \right) 2\pi p^{-(p+3)/2} \right)^{1/p}. \quad (64)$$

Since this is finite for all  $1 \leq p$ , we conclude that  $\mathcal{F}(t) : L^q \rightarrow L^s$  is bounded for any  $1 \leq q \leq s$  and thus  $f \in L^q$  implies  $\mathcal{F}(t)f \in L^{[q, \infty]}$ .

The bounds (63) and (64) indicate the function spaces in which the results live, but do not provide an understanding of the sizes of the results. We now analyze the expected sizes. Our analysis is based on expected scalings, and so provides understanding and estimates, but not rigorous bounds. As described in Sec. I A,  $\mathcal{F}(t)$  is used when we replace  $\tilde{\Phi}$  with  $\mathcal{F}(t)\tilde{\Phi}$  and then again applied at the end of (21), where it appears along with a scalar as  $|\mathbb{E}(t)|\mathcal{F}(t)$ . The matrix  $\mathbb{E}(t)$  is constructed from the matrix  $\mathbb{L}(t) = \mathbb{L}(\mathcal{F}(t)\tilde{\Phi}, \Phi)$ , which has entries of the form  $\langle \mathcal{F}(t)\tilde{\Phi}, \phi \rangle$  and thus satisfy  $|\langle \mathcal{F}(t)\tilde{\Phi}, \phi \rangle| \leq \|\mathcal{F}(t)\tilde{\Phi}\|_2 \|\phi\|_2 \leq \|F(t)\|_1 \|\tilde{\Phi}\|_2 \|\phi\|_2$ . The scaling is thus  $|\mathbb{L}(t)| \sim \|F(t)\|_1^N$  and since  $\mathbb{E}(t)$  is formed by replacing one row of  $\mathbb{L}(t)$  with an orthonormal vector, its scaling is  $|\mathbb{E}(t)| \sim \|F(t)\|_1^{N-1}$ . Using  $\|F(t)\|_1 = (\exp(-e^t + t)/(-\mu))^{1/N}$  from (63), we can incorporate this scaling and obtain the estimates

$$\|\mathbb{E}(t)|F(t)\|_p \sim \|F(t)\|_1^{N-1} \|F(t)\|_p = [(63) \text{ with } N = 1] \quad \text{and} \quad (65)$$

$$\|\nabla|\mathbb{E}(t)|F(t)\|_p \sim \|F(t)\|_1^{N-1} \|\nabla F(t)\|_p = [(64) \text{ with } N = 1]. \quad (66)$$

These estimates have removed the dependence on  $N$ , but leave a dependence on  $t$ . To remove this dependence, we integrate over  $t$  and apply (56) to obtain

$$\int_{-\infty}^{\infty} \|\mathbb{E}(t)|F(t)\|_p dt \sim \left( \frac{1}{-\mu} \right) \left( \frac{-\mu}{2\pi} \right)^{3/2} \left( \frac{-\mu p}{2\pi} \right)^{-3/(2p)} \Gamma \left( \frac{3-p}{2p} \right) \quad \text{for } 1 \leq p < 3 \text{ and} \quad (67)$$

$$\int_{-\infty}^{\infty} \|\nabla|\mathbb{E}(t)|F(t)\|_p dt \sim \left( \frac{2}{-\mu} \right)^{1/(2p)} \pi^{-3/2} \left( \Gamma \left( \frac{p+3}{2} \right) 2\pi p^{-(p+3)/2} \right)^{1/p} \Gamma \left( \frac{1}{2p} \right). \quad (68)$$

It does not quite make sense to integrate these operator norms in this way, since the functions that  $|\mathbb{E}(t)|\mathcal{F}(t)$  are applied to also depend on  $t$ . Nonetheless, to understand the sizes of objects that we encounter, we will lump all these operators together into a single  $\mathcal{F}$  and use (67) and (68) as its bounds. Due to the restriction  $p < 3$  in (67), the operator norm of  $\mathcal{F} : L^q \rightarrow L^s$  is only finite when  $p = (1 + 1/s - 1/q)^{-1} < 3 \Rightarrow q \geq 3s/(3 + 2s)$ . If  $3/2 \leq q$ , then this imposes no additional restriction on  $s$  and we have  $f \in L^q$  implies  $\mathcal{F}f \in L^{[q, \infty]}$ ; however,  $q < 3/2 \Rightarrow s < 3q/(3 - 2q)$  so we only have  $\mathcal{F}f \in L^{[q, 3q/(3-2q))}$ .

#### 4. Ensuring accuracy in the Green function

We now consider how to discretize (61) to obtain a sufficiently accurate approximation for  $\mathcal{G}_\mu$  as a sum of separable convolutions with Gaussians. We require  $L^\infty$  relative error for  $\hat{G}_\mu$  in (58) bounded by  $\epsilon$ . By the isometry of the Fourier transform this gives relative error bounded by  $\epsilon$  for  $G_\mu : L^2(\mathbf{R}^{3N}) \rightarrow L^2(\mathbf{R}^{3N})$ , which is sufficient to run the Green function iteration in Sec. I A and all that we required in Ref. 3.

The analysis in Sec. II C 3 showed that accuracy requirements for  $\mathcal{F} : L^q \rightarrow L^s$  correspond to accuracy requirements for  $G_\mu : L^q \rightarrow L^s$  for  $N = 1$ . Our requirement above for  $L^\infty$  relative error for  $\hat{G}_\mu$  thus provides relative error control for  $\mathcal{F} : L^2 \rightarrow L^2$ . Anticipating our later needs, we will also require  $L^2$  relative error for  $\hat{G}_\mu$  for  $N = 1$  bounded by  $\epsilon$ . By the isometry of the Fourier transform and Young's inequality (51), this provides error control  $\mathcal{F} : L^q \rightarrow L^s$  for  $1/q = 1/s + 1/2$ . Since we normalize by the  $L^2$  norm of the kernel rather than the operator norm of  $\mathcal{G}_\mu$  (which we cannot

compute) and Young's inequality may not be sharp, this does not quite provide relative error in operator norm but should only be off by a small constant.

Following Ref. 13, we will truncate the domain of integration in (59) to  $[-A, B]$  with  $-A < 0 < B$  and there approximate the integral with the trapezoid rule with step size  $h$ . To achieve pointwise relative error in (59) bounded by  $\epsilon$ , the proof of Theorem 3 in Ref. 13 shows it is sufficient to set

$$h < \frac{2\pi\theta}{\ln(1 + 2/(\epsilon \cos \theta))} \quad (69)$$

for any  $0 < \theta < \pi/2$ . In order to get a simple expression, they then select  $\theta = 1$  and bound the denominator from above. There does not appear to be a closed formula for the  $\theta$  that maximizes (69) for a given  $\epsilon$ , but it is simple to numerically maximize this function, so that is what we will do. We observe that  $\theta \rightarrow (\pi/2)^-$  as  $\epsilon \rightarrow 0^+$ . Since (60) is obtained from (59) by substitution, we therefore also obtain pointwise relative error bounded by  $\epsilon$  in (60) and thus  $L^\infty$  and  $L^2$  relative error for  $\hat{G}_\mu$  bounded by  $\epsilon$ .

Truncating the infinite integral (59) to an integral on the interval  $[-A, B]$  has three effects on the accuracy of the approximation. First, neglecting  $(B, \infty)$  means the approximation will go to a finite limit as  $z \rightarrow 0^+$  and thus for small  $z$  the pointwise error will also go to  $z^{-1}$ . Second, neglecting  $(-\infty, -A)$  means the approximation will go to zero much faster than  $z^{-1}$  for large  $z$ , and thus for large  $z$  the pointwise error will go to  $z^{-1}$ . Third, neglecting these intervals will cause some pointwise relative error for intermediate  $z$ .

The pointwise relative error in (59) from neglecting  $0 < B < s < \infty$  is bounded by

$$z \int_B^\infty \exp(-ze^t + t) dt = z \int_{\exp(B)}^\infty e^{-zs} ds = \exp(-ze^B), \quad (70)$$

so to make it at most  $\epsilon$  we need  $B > \ln(-\ln(\epsilon)/z)$ . Since we will substitute  $z = (2\pi^2\|\mathbf{z}\|^2 - \mu)/(-\mu) \geq 1$ , it suffices to take  $B > \ln(-\ln(\epsilon))$ .

The pointwise relative error in (59) from neglecting  $-\infty < s < -A < 0$  is given by

$$z \int_{-\infty}^{-A} \exp(-ze^t + t) dt = z \int_0^{\exp(-A)} e^{-zs} ds = 1 - \exp(-ze^{-A}), \quad (71)$$

so to make it at most  $\epsilon$  we need  $A > -\ln(-\ln(1 - \epsilon)/z) \approx -\ln(\epsilon/z)$ . If we fix some  $Z > 0$  and choose  $A = -\ln(-\ln(1 - \epsilon)/Z)$ , then our approximation has pointwise relative error at most  $\epsilon$  for  $0 < z < Z$  and this propagates to pointwise and normwise relative error for  $\hat{G}_\mu$ . Since the integrand in (59) is positive, the pointwise (not relative) error for  $Z < z$  is bounded by  $1/z$ . The pointwise error in  $\hat{G}_\mu(\mathbf{z})$  via (60) for  $Z < z = (2\pi^2\|\mathbf{z}\|^2 - \mu)/(-\mu)$  is then bounded by  $(-\mu Z)^{-1}$ . Relative to  $\|\hat{G}_\mu\|_\infty = (-\mu)^{-1}$  this gives pointwise error at most  $Z^{-1}$ . Thus we can achieve relative error in  $L^\infty$  for  $\hat{G}_\mu$  as long as  $Z > \epsilon^{-1}$ , which means  $A > -\ln(-\ln(1 - \epsilon)\epsilon) \approx -2\ln(\epsilon)$ . To bound the  $L^2$  norm of the error for  $Z < z$  we explicitly compute the  $L^2$  norm of  $\hat{G}_\mu$  for  $Z < z$  when  $N = 1$ . Since  $\hat{G}_\mu$  is radial, setting  $S = [(-\mu)(Z - 1)/(2\pi^2)]^{1/2}$  we have

$$\left[ 4\pi \int_S^\infty \left( \frac{1}{2\pi^2 s^2 - \mu} \right)^2 s^2 ds \right]^{1/2} \quad (72)$$

$$= \left[ \frac{1}{2} \frac{1}{\sqrt{(-\mu)(2\pi^2)}} - \frac{1}{\pi \sqrt{(-\mu)(2\pi^2)}} \left( -\frac{(Z-1)^{1/2}}{Z} + \arctan((Z-1)^{1/2}) \right) \right]^{1/2}. \quad (73)$$

For large arguments,  $Z - 1 \approx Z$  and  $\arctan(x) \approx \pi/2 - x^{-1}$  so we have

$$\left[ \frac{1}{2} \frac{1}{\sqrt{(-\mu)(2\pi^2)}} - \frac{1}{\pi \sqrt{(-\mu)(2\pi^2)}} (-Z^{-1/2} + (\pi/2 - Z^{-1/2})) \right]^{1/2} = \left[ \frac{\sqrt{2}}{\pi^2 \sqrt{(-\mu)Z}} \right]^{1/2}. \quad (74)$$

Dividing by  $\|G_\mu\|_2 = \pi^{-1/2} 2^{-3/4} (-\mu)^{-1/4}$  gives relative error  $2\pi^{-1/2} Z^{-1/4}$ . Thus to achieve relative error  $\epsilon$  we must choose  $Z > 2^4 \pi^{-2} \epsilon^{-4}$ , which means  $A > -\ln(-\ln(1 - \epsilon) 2^{-4} \pi^2 \epsilon^4) \approx -5\ln(\epsilon) + 2\ln(4/\pi)$ .

### III. OPERATION DIAGRAM ANALYSIS

#### A. Function space inequalities and calculations

Minkowski's inequality states

$$\|f + g\|_p \leq \|f\|_p + \|g\|_p \quad \text{for } 1 \leq p \leq \infty. \quad (75)$$

(When  $p = 2$  this is the Schwarz inequality; it is sometimes called the triangle inequality.) As an application of (32), for  $1 \leq s \leq \infty$  and  $1/p + 1/q = 1$  we have

$$\|fg\|_s = (\langle |f|^s, |g|^s \rangle)^{1/s} \leq \| |f|^s \|_p^{1/s} \| |g|^s \|_q^{1/s} = \|f\|_{ps} \|g\|_{qs} \quad (76)$$

and in particular choosing  $p = \infty \Rightarrow q = 1$  we have

$$\|fg\|_s \leq \|f\|_\infty \|g\|_s. \quad (77)$$

As a second application of (32), for  $1 \leq s \leq \infty$ ,  $0 < t < 1$ ,  $1 \leq stp$ ,  $1 \leq s(1-t)q$ , and  $1/p + 1/q = 1$  we have

$$\|f\|_s = (\langle |f|^{ts}, |f|^{(1-t)s} \rangle)^{1/s} \leq \| |f|^{ts} \|_p^{1/s} \| |f|^{(1-t)s} \|_q^{1/s} = \|f\|_{stp}^t \|f\|_{s(1-t)q}^{1-t}. \quad (78)$$

For  $a \leq s \leq b$  we can set  $a = stp$  and  $b = s(1-t)q$  and solve to obtain

$$\|f\|_s \leq \left( \|f\|_a^{a(b-s)} \|f\|_b^{b(s-a)} \right)^{1/(s(b-a))}, \quad (79)$$

which in particular shows the embedding

$$L^a \cap L^b \subset L^s. \quad (80)$$

In  $d = 3$  we can explicitly compute the  $L^p$  norms of the function  $1/\|\mathbf{r}\|$  restricted to the inside or outside of a sphere of radius  $t$  via

$$\left\| \frac{1}{\|\mathbf{r}\|} \right\|_{\|\mathbf{r}\| \leq t}^p = \left( 4\pi \int_0^t \frac{1}{r^p} r^2 dr \right)^{1/p} = \left( \frac{4\pi t^{3-p}}{3-p} \right)^{1/p} \quad \text{for } 1 \leq p < 3 \text{ and} \quad (81)$$

$$\left\| \frac{1}{\|\mathbf{r}\|} \right\|_{t < \|\mathbf{r}\|}^p = \left( 4\pi \int_t^\infty \frac{1}{r^p} r^2 dr \right)^{1/p} = \begin{cases} (4\pi t^{3-p}/(p-3))^{1/p} & \text{for } 3 < p < \infty \\ t^{-1} & \text{for } p = \infty \end{cases}. \quad (82)$$

For  $p$  not in the specified ranges, the norms are infinite; note that no  $p$  works for both the inside and outside portions.

We shall several times wish to minimize a function of the form  $f(t) = At^p + Bt^{-q}$  with  $A, B, p, q, t > 0$ . Computing the derivative and setting equal to zero yields

$$t_0 = \left( \frac{Bq}{Ap} \right)^{\frac{1}{p+q}} \quad \text{and} \quad (83)$$

$$f(t_0) = (p+q) \left( \frac{A}{q} \right)^{\frac{q}{p+q}} \left( \frac{B}{p} \right)^{\frac{p}{p+q}}. \quad (84)$$

#### B. Analysis using $L^2$

In this section, we assume only that the input functions are in  $L^2$ , and demonstrate the function space diagram (23). Although this diagram fails to provide error bounds, the analysis is enlightening.

##### 1. Product

Using (76) with  $s = 1$  and  $p = q = 2$  we have

$$\|\phi\theta\|_1 \leq \|\phi\|_2 \|\theta\|_2 \quad (85)$$

and thus  $\phi\theta \in L^1$ . If we only know that  $\phi$  and  $\theta$  are in  $L^2$ , then no bound holds for  $\|\phi\theta\|_p$  for  $1 < p$ . For example, if  $\phi$  and  $\theta$  both have value  $\sqrt{C}$  on a ball of volume  $1/C$  around a nucleus and are zero elsewhere, then  $\|\phi\|_2 = \|\theta\|_2 = 1$ , but  $\|\phi\theta\|_p = C^{(p-1)/p} \rightarrow \infty$  as  $C \rightarrow \infty$ .

## 2. Nuclear potential

We first show that  $\phi\theta \in L^1$  provides no bound on  $\langle V, \phi\theta \rangle$ , even for the case of a single nucleus at the origin. Let  $\phi\theta$  have value  $C$  on a ball of volume  $1/C$  around a nucleus and zero elsewhere, so  $\|\phi\theta\|_1 = 1$ . We can explicitly compute using (81) that

$$\langle V, \phi\theta \rangle = CZ \left\| \frac{1}{\|\mathbf{r}\|} \right\|_{\|\mathbf{r}\| \leq (3/(4\pi C))^{1/3}} = C^{1/3} Z \pi^{1/3} 3^{2/3} 2^{-1/3}, \quad (86)$$

which diverges as  $C \rightarrow \infty$ .

Next we show that  $\phi \in L^2$  provides no bound for  $\|V\phi\|_p$  for any  $1 \leq p$ , even for the case of a single nucleus at the origin. Let  $\phi$  have value  $\sqrt{C}$  on a ball of volume  $1/C$  around a nucleus and zero elsewhere, so  $\|\phi\|_2 = 1$ . We can then compute using (81) that

$$\|V\phi\|_r = C^{1/2} Z \left\| \frac{1}{\|\mathbf{r}\|} \right\|_{\|\mathbf{r}\| \leq (3/(4\pi C))^{1/3}} = C^{(5r-6)/(6r)} Z 4^{1/3} \pi^{1/3} 3^{(3-r)/(3r)} (3-r)^{-1/r}. \quad (87)$$

If  $6/5 < r$ , then this diverges as  $C \rightarrow \infty$  and if  $r < 6/5$  it diverges as  $C \rightarrow 0$ . For  $r = 6/5$  the construction is a little more difficult. Let  $\phi$  have value  $r^t (4\pi)^{-1/2}$  on the ball of radius  $(3 + 2t)^{1/(3+2t)}$  for some  $-3/2 < t$ . Then

$$\|\phi\|_2 = \left( 4\pi \int_0^{(3+2t)^{1/(3+2t)}} \frac{r^{2t}}{4\pi} r^2 dr \right)^{1/2} = \left( \frac{r^{3+2t}}{3+2t} \Big|_0^{(3+2t)^{1/(3+2t)}} \right)^{1/2} = 1 \quad \text{and} \quad (88)$$

$$\begin{aligned} \|V\phi\|_{6/5} &= Z \left( 4\pi \int_0^{(3+2t)^{1/(3+2t)}} \frac{r^{(6/5)t}}{(4\pi)^{3/5}} r^{2-6/5} dr \right)^{5/6} \\ &= Z (4\pi)^{1/3} \left( \frac{r^{(9/5)+(6/5)t}}{(9/5)+(6/5)t} \Big|_0^{(3+2t)^{1/(3+2t)}} \right)^{5/6} \\ &= Z (4\pi)^{1/3} \left( \frac{(3+2t)^{3/5}}{(3/5)(3+2t)} \right)^{5/6} = Z (4\pi)^{1/3} (5/3)^{5/6} (3+2t)^{-1/3}, \end{aligned} \quad (89)$$

which diverges as  $t \rightarrow (-3/2)^+$ .

## 3. Poisson convolution

We first show  $\phi\theta \in L^1$  provides no bound on  $\|\mathcal{W}_p[\phi\theta]\|_p$  for any  $1 \leq p$ . Let  $\phi\theta$  have value  $C$  on a ball of volume  $1/C$  around a nucleus and zero elsewhere, so  $\|\phi\theta\|_1 = 1$ . For  $\|\mathbf{r}\| \leq (3/(4\pi C))^{1/3}/2$  we have

$$\mathcal{W}_p[\phi\theta](\mathbf{r}) \geq C \left\| \frac{1}{\|\mathbf{r}\|} \right\|_{\|\mathbf{r}\| \leq (3/(4\pi C))^{1/3}/2} = C \frac{4\pi(3/(4\pi C))^{2/3} 2^{-2}}{2} = C^{1/3} \pi^{1/3} 3^{2/3} 2^{-7/3}, \quad (90)$$

and thus

$$\|\mathcal{W}_p[\phi\theta]\|_p \geq C^{1/3} \pi^{1/3} 3^{2/3} 2^{-7/3} (8C)^{-1/p} = C^{(p-3)/(3p)} \pi^{1/3} 3^{2/3} 2^{(9-7p)/(3p)}. \quad (91)$$

If  $p < 3$ , then this diverges as  $C \rightarrow 0$  and if  $3 < p$ , then this diverges as  $C \rightarrow \infty$ . Now let  $C = 3/(4\pi)$  so the ball has radius 1. We then have  $\mathcal{W}_p[\phi\theta](\mathbf{r}) \geq 1/(1 + \|\mathbf{r}\|)$ , so  $\mathcal{W}_p[\phi\theta]$  cannot be in  $L^p$  for any  $p \leq 3$ . Thus we conclude  $\mathcal{W}_p[\phi\theta]$  cannot be in  $L^p$  for any  $p$ .

Next we show  $\phi\theta, \tilde{\phi}\tilde{\theta} \in L^1$  provides no bound on  $\langle \tilde{\phi}\tilde{\theta}, \mathcal{W}_P[\phi\theta] \rangle$ . Let both  $\phi\theta$  and  $\tilde{\phi}\tilde{\theta}$  have value  $C$  on a ball of volume  $1/C$  around a nucleus and zero elsewhere, so  $\|\phi\theta\|_1 = \|\tilde{\phi}\tilde{\theta}\|_1 = 1$ . Then by (90),

$$\begin{aligned} \langle \tilde{\phi}\tilde{\theta}, \mathcal{W}_P[\phi\theta] \rangle &\geq \int_{\|\mathbf{r}\| \leq (3/(4\pi C))^{1/3}/2} C C^{1/3} \pi^{1/3} 3^{2/3} 2^{-7/3} d\mathbf{r} \\ &= \pi^{4/3} 3^{2/3} 2^{-1/3} C^{4/3} \frac{r^3}{3} \Big|_0^{(3/(4\pi C))^{1/3}/2} = \pi^{1/3} 3^{2/3} 2^{-4/3} C^{1/3}, \end{aligned} \quad (92)$$

which diverges as  $C \rightarrow \infty$ .

### C. Analysis using $L^{[2, u]}$ for $3 < u$

In this section, we demonstrate the diagram (26) for  $3 < u \leq \infty$ . For  $\|V\phi\|_s$  the form of the bound changes at  $u = 6$  but we only give the details for  $3 < u \leq 6$ .

#### 1. Product

In Sec. III B 1, we showed that  $\phi\theta \in L^1$  since  $\phi$  and  $\theta$  are in  $L^2$ . Using (76) we have

$$\|\phi\theta\|_{u/2} \leq \|\phi\|_u \|\theta\|_u \quad (93)$$

and thus  $\phi$  and  $\theta$  in  $L^u$  implies  $\phi\theta \in L^{u/2}$ . Applying (78) with  $stp = 1$  and  $s(1 - t)q = u/2$  and thus  $t = (u - 2s)/(s(u - 2))$  yields for  $1 \leq s \leq u/2$  that

$$\|\phi\theta\|_s \leq \|\phi\theta\|_1^{(u-2s)/(s(u-2))} \|\phi\theta\|_{u/2}^{(s-1)u/(s(u-2))} \quad (94)$$

and so  $\phi\theta \in L^{[1, u/2]}$ .

#### 2. Nuclear potential

Select some  $C_v > 0$  and split  $V = V_{\text{near}} + V_{\text{far}}$  with

$$V_{\text{near}}(\mathbf{r}) = \begin{cases} V(\mathbf{r}) & \text{if } V(\mathbf{r}) \geq C_v \\ 0 & \text{if } V(\mathbf{r}) < C_v \end{cases} \quad \text{and} \quad V_{\text{far}}(\mathbf{r}) = \begin{cases} 0 & \text{if } V(\mathbf{r}) \geq C_v \\ V(\mathbf{r}) & \text{if } V(\mathbf{r}) < C_v \end{cases}. \quad (95)$$

For a single nucleus of charge  $Z$  we have via (81) and (82),

$$\|V_{\text{near}}\|_p = Z \left\| \frac{1}{\|\mathbf{r}\|} \Big|_{\|\mathbf{r}\| \leq Z/C_v} \right\|_p = \left( \frac{4\pi Z^3}{(3-p)C_v^{3-p}} \right)^{1/p} \quad \text{for } 1 \leq p < 3 \quad \text{and} \quad (96)$$

$$\|V_{\text{far}}\|_p = Z \left\| \frac{1}{\|\mathbf{r}\|} \Big|_{Z/C_v < \|\mathbf{r}\|} \right\|_p = \begin{cases} (4\pi Z^3 C_v^{p-3}/(p-3))^{1/p} & \text{for } 3 < p < \infty \\ C_v & \text{for } p = \infty \end{cases}. \quad (97)$$

For  $p$  outside the given ranges the norms are infinite. In particular, the motivation to split  $V$  is that no  $p$  gives finite value for both (96) and (97). Now suppose  $V$  comes from a collection of nuclei with total charge  $\sum_i Z_i = Z_{\text{total}}$ . If they are at infinite distance we obtain norms  $\sim (\sum_i Z_i^3)^{1/p}$ , whereas if they coalesce to a single nucleus we obtain  $\sim (\sum_i Z_i)^{3/p}$ , so a single nucleus gives the largest value, and we have the bounds

$$\|V_{\text{near}}\|_p \leq \left( \frac{4\pi Z_{\text{total}}^3}{(3-p)C_v^{3-p}} \right)^{1/p} \quad \text{for } 1 \leq p < 3 \quad \text{and} \quad (98)$$

$$\|V_{\text{far}}\|_p \leq \begin{cases} (4\pi Z_{\text{total}}^3 C_v^{p-3}/(p-3))^{1/p} & \text{for } 3 < p < \infty \\ C_v & \text{for } p = \infty \end{cases}. \quad (99)$$

Splitting into near and far parts and applying (32) separately with  $(L^p, L^{p/(p-1)})$  and  $(L^q, L^{q/(q-1)})$  to the pieces, we obtain

$$|\langle V, \phi\theta \rangle| \leq |\langle V_{\text{near}}, \phi\theta \rangle| + |\langle V_{\text{far}}, \phi\theta \rangle| \leq \|V_{\text{near}}\|_p \|\phi\theta\|_{p/(p-1)} + \|V_{\text{far}}\|_q \|\phi\theta\|_{q/(q-1)}. \quad (100)$$

We now try to choose  $p$  and  $q$  to make all terms finite. Choosing the extremal values  $q/(q-1) = 1 \Rightarrow q = \infty$  and  $p/(p-1) = u/2 \Rightarrow p = u/(u-2)$  and using (98) and (99), we then obtain

$$\begin{aligned} |\langle V, \phi\theta \rangle| &\leq \|V_{\text{near}}\|_{u/(u-2)} \|\phi\theta\|_{u/2} + \|V_{\text{far}}\|_{\infty} \|\phi\theta\|_1 \\ &= C_v^{(6-2u)/u} \left( \frac{(u-2)4\pi Z_{\text{total}}^3}{(2u-6)} \right)^{(u-2)/u} \|\phi\theta\|_{u/2} + C_v \|\phi\theta\|_1. \end{aligned} \quad (101)$$

Since  $\|V_{\text{near}}\|_p$  is only bounded for  $1 \leq p < 3$ , we must have  $u/(u-2) < 3 \Rightarrow 3 < u$ , which we assumed. Using (83), the quantity (101) is minimized by choosing

$$C_v = Z_{\text{total}} \left( \frac{(u-2)4\pi}{(2u-6)} \right)^{1/3} \left( \frac{(2u-6)}{u} \right)^{u/(3u-6)} \left( \frac{\|\phi\theta\|_{u/2}}{\|\phi\theta\|_1} \right)^{u/(3u-6)} \quad (102)$$

and then yields the bound

$$|\langle V, \phi\theta \rangle| \leq Z_{\text{total}} \pi^{1/3} 3 \left( \frac{2(u-2)^4}{u^3(u-3)} \right)^{1/3} \left( \frac{u}{2(u-3)} \right)^{(2u-6)/(3u-6)} \|\phi\theta\|_1^{(2u-6)/(3u-6)} \|\phi\theta\|_{u/2}^{u/(3u-6)}. \quad (103)$$

Applying Minkowski's inequality (75) and then (76) to the two pieces, we obtain

$$\begin{aligned} \|V\phi\|_s &\leq \|V_{\text{near}}\phi\|_s + \|V_{\text{far}}\phi\|_s \leq \|V_{\text{near}}\|_{sp} \|\phi\|_{sp/(p-1)} + \|V_{\text{far}}\|_{sq} \|\phi\|_{sq/(q-1)} \\ &\leq \left( \frac{4\pi Z_{\text{total}}^3}{(3-sp)C_v^{3-sp}} \right)^{1/(sp)} \|\phi\|_{sp/(p-1)} + \left\{ \begin{array}{l} \left( 4\pi Z_{\text{total}}^3 C_v^{sq-3}/(sq-3) \right)^{1/(sq)} \\ C_v \quad \text{for } q = \infty \end{array} \right\} \|\phi\|_{sq/(q-1)} \end{aligned} \quad (104)$$

with the restrictions that  $1 \leq p \leq \infty$ ,  $1 \leq q \leq \infty$ ,  $1 \leq s \leq \infty$ ,  $1 \leq sp < 3$ , and  $3 < sq \leq \infty$ . The restrictions  $1 \leq p \leq \infty$  and  $1 \leq sp < 3$  immediately restrict our consideration to  $1 \leq s < 3$ . The restriction  $1 \leq sp < 3$  has least effect on  $s$  when we choose  $p$  as small as possible, which means  $sp/(p-1)$  as large as possible, so we choose  $sp/(p-1) = u \Rightarrow sp = us/(u-s)$  and we have the restriction  $us/(u-s) < 3 \Rightarrow s < 3u/(3+u)$ . The restriction  $3 < sq \leq \infty$  has least effect on  $s$  when we choose  $q$  as large as possible, which means  $sq/(q-1)$  as small as possible, which is  $\max\{s, 2\}$ . If  $s < 2$ , then we choose  $sq/(q-1) = 2 \Rightarrow sq = 2s/(2-s)$  and so have the restriction  $3 < 2s/(2-s) \Rightarrow 6/5 < s$ . If  $2 \leq s$ , then we can choose  $q = \infty$  and use  $\|\phi\|_s$ ; note that  $u \leq 6 \Rightarrow s < 3u/(3+u) < 2$  and then this case cannot occur. Thus we obtain  $V\phi \in L^{(6/5, 3u/(3+u))}$  and for  $u \leq 6$  the bound

$$\|V\phi\|_s \leq C_v^{-(3u-3s-us)/(us)} \left( \frac{4\pi Z_{\text{total}}^3(u-s)}{(3u-3s-us)} \right)^{\frac{u-s}{us}} \|\phi\|_u + C_v^{(5s-6)/(2s)} \left( \frac{4\pi Z_{\text{total}}^3(2-s)}{(5s-6)} \right)^{\frac{2-s}{2s}} \|\phi\|_2. \quad (105)$$

Using (83), the quantity (105) is minimized by choosing

$$C_v = 2^{2/3} \pi^{1/3} Z_{\text{total}} \left( \frac{u-s}{3u-3s-us} \right)^{\frac{2(u-s)}{3s(u-2)}} \left( \frac{2-s}{5s-6} \right)^{-\frac{u(2-s)}{3s(u-2)}} \left( \frac{2(3u-3s-us)}{u(5s-6)} \right)^{\frac{2u}{3u-6}} \left( \frac{\|\phi\|_u}{\|\phi\|_2} \right)^{\frac{2u}{3u-6}} \quad (106)$$

and then yields the bound

$$\begin{aligned} \|V\phi\|_s &\leq \frac{Z_{\text{total}} 3s(u-2)}{(3u-3s-us)} \left( \frac{\pi(2-s)}{2(5s-6)} \right)^{1/3} \left( \frac{(u-s)(5s-6)}{(2-s)(3u-3s-us)} \right)^{\frac{(u-s)(5s-6)}{3s^2(u-2)}} \left( \frac{2(3u-3s-us)}{u(5s-6)} \right)^{\frac{u(5s-6)}{3s(u-2)}} \\ &\quad \times \|\phi\|_2^{2(3u-3s-us)/(3s(u-2))} \|\phi\|_u^{u(5s-6)/(3s(u-2))}. \end{aligned} \quad (107)$$

### 3. Poisson convolution

We split  $\mathcal{W}_{\mathcal{P}}[\cdot]$  at some radius  $C_w$  into

$$\mathcal{W}_{\mathcal{P}}[f]_{\text{near}} = \frac{1}{\|\mathbf{r}\|} \Big|_{\|\mathbf{r}\| \leq C_w} * f \quad \text{and} \quad \mathcal{W}_{\mathcal{P}}[f]_{\text{far}} = \frac{1}{\|\mathbf{r}\|} \Big|_{C_w < \|\mathbf{r}\|} * f \quad (108)$$

and read the  $L^p$  norms of the kernels from (81) and (82) as

$$\left\| \frac{1}{\|\mathbf{r}\|} \Big|_{\|\mathbf{r}\| \leq C_w} \right\|_p = \left( \frac{4\pi C_w^{3-p}}{3-p} \right)^{1/p} \quad \text{for } 1 \leq p < 3 \text{ and} \quad (109)$$

$$\left\| \frac{1}{\|\mathbf{r}\|} \Big|_{C_w < \|\mathbf{r}\|} \right\|_p = \begin{cases} \left( \frac{4\pi C_w^{3-p}}{p-3} \right)^{1/p} & \text{for } 3 < p < \infty \\ C_w^{-1} & \text{for } p = \infty \end{cases}. \quad (110)$$

The fact that no single  $p$  gives a finite result for both parts of the kernel is the motivation for splitting the kernel.

Using Minkowski's inequality (75) and then Young's inequality (51) on each piece, we obtain

$$\begin{aligned} \|\mathcal{W}_{\mathcal{P}}[\phi\theta]\|_s &\leq \|\mathcal{W}_{\mathcal{P}}[\phi\theta]_{\text{near}}\|_s + \|\mathcal{W}_{\mathcal{P}}[\phi\theta]_{\text{far}}\|_s \\ &\leq \left\| \frac{1}{\|\mathbf{r}\|} \Big|_{\|\mathbf{r}\| \leq C_w} \right\|_p \|\phi\theta\|_{sp/(sp+p-s)} + \left\| \frac{1}{\|\mathbf{r}\|} \Big|_{C_w < \|\mathbf{r}\|} \right\|_q \|\phi\theta\|_{sq/(sq+q-s)} \end{aligned} \quad (111)$$

with the restrictions that  $1 \leq p < 3 < q \leq \infty$ ,  $1 \leq s \leq \infty$ ,  $1 \leq sp/(sp+p-s)$ , and  $1 \leq sq/(sq+q-s)$ . Since  $1 \leq sp/(sp+p-s) \Rightarrow p \leq s$  and  $1 \leq sq/(sq+q-s) \Rightarrow q \leq s$ , we must have  $3 < s \leq \infty$  and so  $\mathcal{W}_{\mathcal{P}}[\phi\theta] \in L^{(3,\infty]}$ . We choose to use the extremal values  $sp/(sp+p-s) = u/2 \Rightarrow p = us/(u+us-2s)$  and  $q/(sq+q-s) = 1 \Rightarrow q = s$ . For  $3 < s < \infty$  we obtain

$$\|\mathcal{W}_{\mathcal{P}}[\phi\theta]\|_s \leq C_w^{(3u+2us-6s)/(us)} \left( \frac{4\pi(u+us-2s)}{3u+2us-6s} \right)^{\frac{u+us-2s}{us}} \|\phi\theta\|_{u/2} + C_w^{(3-s)/s} \left( \frac{4\pi}{s-3} \right)^{1/s} \|\phi\theta\|_1, \quad (112)$$

which is minimized using (83) by choosing

$$C_w = \left( \left( \frac{4\pi}{s-3} \right)^{1/s} \left( \frac{4\pi(u+us-2s)}{3u+2us-6s} \right)^{-\frac{u+us-2s}{us}} \frac{(s-3)u}{(3u+2us-6s)} \right)^{u/(3u-6)} \left( \frac{\|\phi\theta\|_1}{\|\phi\theta\|_{u/2}} \right)^{u/(3u-6)} \quad (113)$$

and then yields the bound

$$\begin{aligned} \|\mathcal{W}_{\mathcal{P}}[\phi\theta]\|_s &\leq \left( \frac{3s(u-2)}{3u+2us-6s} \right) \left( \frac{4\pi}{s-3} \right)^{1/3} \left( \frac{(s-3)(u+us-2s)}{3u+2us-6s} \right)^{\frac{(u+us-2s)(s-3)}{3s^2(u-2)}} \left( \frac{3u+2us-6s}{u(s-3)} \right)^{\frac{u(s-3)}{3s(u-2)}} \\ &\quad \times \|\phi\theta\|_{u/2}^{u(s-3)/(3s(u-2))} \|\phi\theta\|_1^{(3u+2us-6s)/(3s(u-2))}. \end{aligned} \quad (114)$$

For  $s = \infty$  we obtain

$$\|\mathcal{W}_{\mathcal{P}}[\phi\theta]\|_{\infty} \leq C_w^{2(u-3)/u} \left( \frac{2\pi(u-2)}{u-3} \right)^{(u-2)/u} \|\phi\theta\|_{u/2} + C_w^{-1} \|\phi\theta\|_1, \quad (115)$$

$$C_w = \left( \frac{u-3}{2\pi(u-2)} \right)^{1/3} \left( \frac{u}{2(u-3)} \right)^{u/(3u-6)} \left( \frac{\|\phi\theta\|_1}{\|\phi\theta\|_{u/2}} \right)^{u/(3u-6)}, \quad \text{and} \quad (116)$$

$$\|\mathcal{W}_{\mathcal{P}}[\phi\theta]\|_{\infty} \leq \left( \frac{3(u-2)}{u} \right) \left( \frac{2\pi(u-2)}{u-3} \right)^{1/3} \left( \frac{u}{2(u-3)} \right)^{2(u-3)/(3u-6)} \|\phi\theta\|_{u/2}^{u/(3u-6)} \|\phi\theta\|_1^{2(u-3)/(3u-6)}. \quad (117)$$

Using (76) we have

$$\|\tilde{\phi}\mathcal{W}_{\mathcal{P}}[\phi\theta]\|_t \leq \|\tilde{\phi}\|_{st/(s-t)} \|\mathcal{W}_{\mathcal{P}}[\phi\theta]\|_s \quad (118)$$

with the restrictions  $1 \leq t$ ,  $t \leq s$ ,  $2 \leq st/(s-t) \leq u$ , and  $3 < s$ . For  $t < 2$  we can solve  $2 \leq st/(s-t) \Rightarrow s(2-t) \leq 2t$  and then substitute in and solve  $3 < s \Rightarrow 3(2-t) < 2t \Rightarrow 6/5 < t$ . For  $2 \leq t$  the inequality  $3(2-t) < 2t$  is not a restriction, but  $st/(s-t) \leq u \Rightarrow ut \leq s(u-t) \Rightarrow t \leq u$ . Thus we obtain  $6/5 < t \leq u$  and  $\tilde{\phi}\mathcal{W}_{\mathcal{P}}[\phi\theta] \in L^{(6/5,u)}$ .

Using Hölder's inequality (32) we have

$$|\langle \tilde{\phi}\tilde{\theta}, \mathcal{W}_{\mathcal{P}}[\phi\theta] \rangle| \leq \|\tilde{\phi}\tilde{\theta}\|_{s/(s-1)} \|\mathcal{W}_{\mathcal{P}}[\phi\theta]\|_s. \quad (119)$$

Since (111) requires  $3 < s \leq \infty$  we have  $1 \leq s/(s-1) < 3/2$ . Since  $\tilde{\phi}\tilde{\theta} \in L^{[1,u/2]} \subset L^{[1,3/2]}$ , we need no additional restrictions on  $s$  to assure (119) is finite.

#### 4. Gaussian convolution

In Secs. III C 2 and III C 3, we showed that  $\langle V, \phi\theta \rangle$  and  $\langle \tilde{\phi}\tilde{\theta}, \mathcal{W}_{\mathcal{P}}[\phi\theta] \rangle$  are bounded,  $V\phi \in L^{(6/5,u/(3+u))}$  and  $\tilde{\phi}\mathcal{W}_{\mathcal{P}}[\phi\theta] \in L^{(6/5,u)}$ . To complete the operations diagram (22) we need only apply the Gaussian convolution  $\mathcal{F}$ . In Sec. II C 3, we showed that to obtain results in  $L^2 \cap L^u$  it is sufficient for the argument to be in  $L^p$  for any  $3u/(3+2u) < p \leq 2$ . Since  $2 < u \Rightarrow 3u/(3+2u) < u/(3+u)$ , we have the required condition.

### D. Analysis using $H^1$

In this section, we assume that the input functions are in  $H^1$ , and demonstrate the function space diagram (24). Most of the results follow from the  $L^{[2,u]}$  results in Sec. III C setting  $u = 6$ .

#### 1. Background results

These results assume  $f \in C_0^\infty(\mathbf{R}^3)$ , but a limiting argument can be used to extend both of them to  $H^1$ .

**Theorem 3.1** (Ref. 14, p. 20 with  $d = 3$ ). Assume that  $f \in C_0^\infty(\mathbf{R}^3)$ , an infinitely differentiable function with compact support. Then for  $1 < p < 3$  and  $q = 3p/(3-p)$ ,

$$\|f\|_q \leq \frac{p-1}{3-p} \left( \frac{3-p}{3(p-1)} \right)^{1/q} \left( \frac{3}{2\pi\Gamma(3/p)\Gamma(4-3/p)} \right)^{1/3} \|\nabla f\|_p, \quad (120)$$

where  $\Gamma$  is defined by (56).

Choosing  $p = 2$  makes  $q = 6$  and yields

$$\|f\|_6 \leq \left( \frac{1}{3} \right)^{1/6} \left( \frac{3}{\Gamma(3/2)\Gamma(5/2)2\pi} \right)^{1/3} \|\nabla f\|_2 = \left( \frac{1}{3} \right)^{1/6} \left( \frac{4}{\pi^2} \right)^{1/3} \|\nabla f\|_2. \quad (121)$$

The following Hardy-type inequality is found in Ref. 15.

**Lemma 3.2.** If  $f \in C_0^\infty(\mathbf{R}^3)$ , then

$$\left\| \frac{1}{\|\mathbf{r}\|} f \right\|_2 \leq 2\|\nabla f\|_2. \quad (122)$$

#### 2. Product

In Sec. III C 1, we showed that  $\phi, \theta \in L^2 \cap L^u$  implies  $\phi\theta \in L^{[1,u/2]}$ . Applying Theorem 3.1 via (121) we have  $\|f\|_6 \leq 3^{-1/6} 4^{1/3} \pi^{-2/3} \|\nabla f\|_2$  and thus  $H^1 \subset L^2 \cap L^6$ . We then have  $\phi\theta \in L^{[1,3]}$  and the bound

$$\|\phi\theta\|_3 \leq \|\phi\|_6 \|\theta\|_6 \leq 3^{-1/3} 4^{2/3} \pi^{-4/3} \|\nabla\phi\|_2 \|\nabla\theta\|_2. \quad (123)$$

### 3. Nuclear potential

Since  $H^1 \subset L^2 \cap L^6$ , the results in Sec. III C 2 hold using  $u = 6$ . Applying (122) and Minkowski's inequality (75), we obtain

$$\|V\phi\|_2 \leq 2Z_{\text{total}} \|\nabla\phi\|_2, \quad (124)$$

and thus we have the stronger result  $V\phi \in L^{(6/5,2]}$ . (The bound (107) on  $\|V\phi\|_s$  with  $u = 6$  goes to infinity as  $s \rightarrow 2^-$  and so is definitely not sharp for  $\phi \in H^1$ ; a better bound can be obtained using (124) and interpolation (78).)

### 4. Poisson convolution

Since  $H^1 \subset L^2 \cap L^6$ , the results in Sec. III C 3 hold with  $u = 6$ . We are not aware that  $H^1$  gives any stronger result.

### 5. Gaussian convolution

To complete the operations diagram (22) we need only apply the Gaussian convolution  $\mathcal{F}$ . In Sec. II C 3, we showed that to obtain final results in  $H^1$  as claimed in (24) it suffices to have the argument for  $\mathcal{F}$  in  $L^p$  for some  $1 \leq p \leq 2$ , which have shown to be true.

## IV. CHOOSING THE FUNCTION SPACES USING THE CORE ORBITAL

In Sec. IV A, we introduce the core orbital and compute exact quantities involving it. In Sec. IV B, we analyze how the choice of function space affects the allowed truncation radius for the various operators. From this analysis we determine that we should choose  $4 \leq u \leq 6$  and  $V\phi \in L^{2u/(u+2)}$ . In Sec. IV C, we test our various bounds on the core orbital using  $u = 4$  and  $u = 6$ . From this analysis we determine that we should choose  $\mathcal{W}_p[\phi\theta] \in L^4$  and  $\tilde{\phi}\mathcal{W}_p[\phi\theta] \in L^2$ . We determine that there are no negatives to choosing  $u = 4$ , so we recommend it.

### A. The core orbital

The core orbital is

$$\varphi(\mathbf{r}) = \sqrt{\frac{Z^3}{\pi}} \exp(-Z\|\mathbf{r}\|), \quad (125)$$

which is the exact solution to the Schrödinger equation with a single nucleus when  $N = 1$ . Explicitly, we have

$$\left(-\frac{1}{2}\nabla^2 - \frac{Z}{\|\mathbf{r}\|}\right)\varphi(\mathbf{r}) = -\frac{1}{2}\left(-\frac{2Z}{\|\mathbf{r}\|} + Z^2\right)\varphi(\mathbf{r}) - \frac{Z}{\|\mathbf{r}\|}\varphi(\mathbf{r}) = -\frac{1}{2}Z^2\varphi(\mathbf{r}). \quad (126)$$

Reading the eigenvalue from (126), we can evaluate

$$-\mu \approx -\lambda = (1/2)Z^2. \quad (127)$$

The primary features of  $\varphi$  to note are that it has a cusp at  $r = 0$  and becomes more concentrated around  $r = 0$  as  $Z$  increases. Since it is a function on  $\mathbf{R}^3$ , we cannot plot it directly. In Figure 1, we plot its radial part and illustrate where its  $L^p$  norm concentrates.

We can compute explicitly that

$$\|\varphi\|_p = \left(4\pi \int_0^\infty \left(\frac{Z^3}{\pi}\right)^{p/2} \exp(-pZr)r^2 dr\right)^{1/p} = (2/p)^{3/p} \pi^{1/p-1/2} Z^{3/2-3/p}, \quad (128)$$

$$\|\varphi\|_2 = 1, \quad (129)$$

$$\|\varphi^2\|_p = \|\varphi\|_{2p}^2 = (1/p)^{3/p} \pi^{1/p-1} Z^{3-3/p}, \quad (130)$$

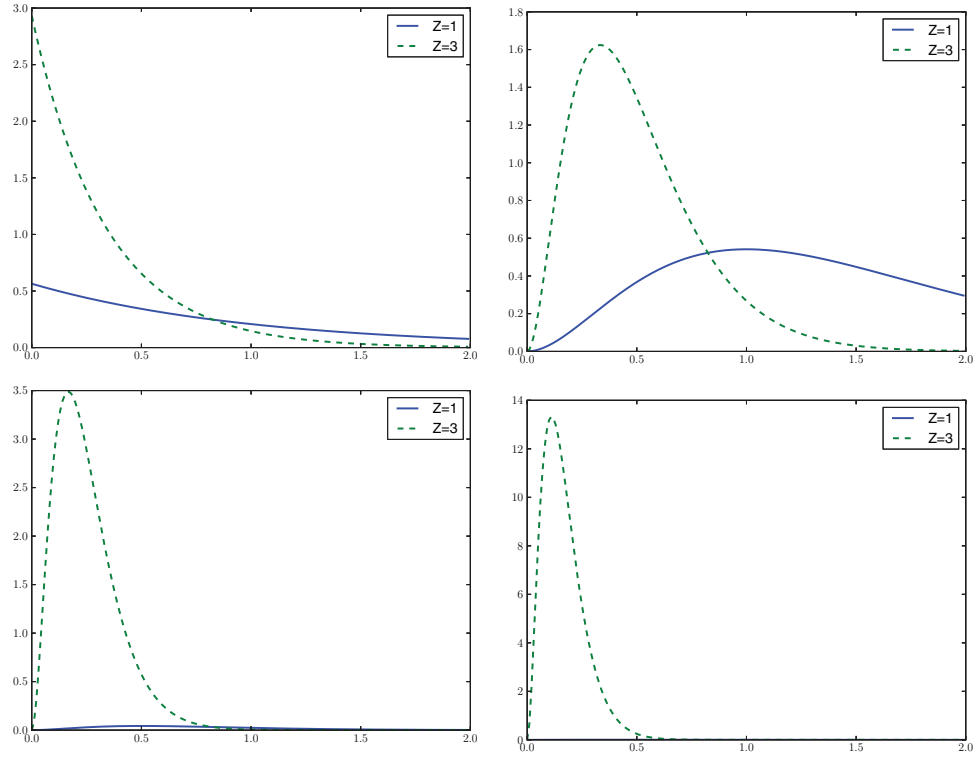


FIG. 1. For  $Z = 1$  and  $Z = 3$ , the radial part of  $\varphi(\mathbf{r})$  (upper left),  $4\pi|\varphi(\mathbf{r})|^2 r^2$  (upper right),  $4\pi|\varphi(\mathbf{r})|^4 r^2$  (lower left), and  $4\pi|\varphi(\mathbf{r})|^6 r^2$  (lower right) for  $0 \leq r \leq 2$ . The latter three illustrate the concentration of the  $L^2$ ,  $L^4$ , and  $L^6$  norms, respectively.

$$\|\varphi^2\|_1 = \|\varphi\|_2^2 = 1, \quad (131)$$

$$\langle V, \varphi^2 \rangle = 4\pi \int_0^\infty -\frac{Z}{r} \frac{Z^3}{\pi} \exp(-2Zr) r^2 dr = -Z^2, \quad \text{and} \quad (132)$$

$$\|\mathcal{W}_P[\varphi^2]\|_\infty = 4\pi \int_0^\infty \frac{1}{r} \frac{Z^3}{\pi} e^{-2Zr} r^2 dr = Z. \quad (133)$$

Using the integral identity (56) we can compute

$$\|V\varphi\|_p = Z \left( 4\pi \int_0^\infty \frac{Z^{3p/2}}{\pi^{p/2}} \exp(-pZr) r^{2-p} dr \right)^{1/p} = Z^{7/2-3/p} 4^{1/p} \pi^{(2-p)/(2p)} p^{1-3/p} \Gamma(3-p)^{1/p}. \quad (134)$$

The last quantity involving  $\mathcal{W}_P[\cdot]$  requires a bit more effort. We have

$$\langle \varphi^2, \mathcal{W}_P[\varphi^2] \rangle = \int \int \frac{Z^3}{\pi} \exp(-2Z\|\mathbf{r}\|) \frac{1}{\|\mathbf{r} - \mathbf{r}'\|} \frac{Z^3}{\pi} \exp(-2Z\|\mathbf{r}'\|) d\mathbf{r}' d\mathbf{r} \quad (135)$$

so using the change of variables  $\mathbf{s} = (Z/\pi)\mathbf{r}$  we have

$$\begin{aligned} & \pi^3 Z \int \exp(-2\pi\|\mathbf{s}\|) \int \exp(-2\pi\|\mathbf{s}'\|) \frac{1}{\|\mathbf{s} - \mathbf{s}'\|} ds' ds \\ &= \pi^3 Z \left\langle \exp(-2\pi\|\mathbf{s}\|), \int \exp(-2\pi\|\mathbf{s}'\|) \frac{1}{\|\mathbf{s} - \mathbf{s}'\|} ds' \right\rangle. \end{aligned} \quad (136)$$

We have the Fourier transform formulas in three dimensions<sup>11</sup>

$$\exp(\widehat{-2\pi\|\mathbf{r}\|})(\xi) = \frac{1}{\pi^2} \frac{1}{(1 + \|\xi\|^2)^2} \quad \text{and} \quad \widehat{\left(\frac{1}{\|\mathbf{r}\|}\right)}(\xi) = \frac{1}{\pi \|\xi\|^2}. \quad (137)$$

Taking Fourier transforms in  $\mathbf{s}$  and using the fact that convolution goes to multiplication, we have

$$\begin{aligned} & \pi^3 Z \left\langle \frac{1}{\pi^2} \frac{1}{(1 + \|\xi\|^2)^2}, \frac{1}{\pi^2} \frac{1}{(1 + \|\xi\|^2)^2} \frac{1}{\pi \|\xi\|^2} \right\rangle \\ &= \frac{Z}{\pi^2} \int \frac{1}{(1 + \|\xi\|^2)^4} \frac{1}{\|\xi\|^2} d\xi = \frac{4Z}{\pi} \int_0^\infty \frac{1}{(1 + x^2)^4} dx. \end{aligned} \quad (138)$$

Using the integral

$$\int \frac{1}{(x^2 + 1)^n} dx = \frac{x}{2(n-1)(x^2 + 1)^{n-1}} + \frac{2n-3}{2(n-1)} \int \frac{1}{(x^2 + 1)^{n-1}} dx \quad (139)$$

from a standard table, we finally obtain

$$\frac{4Z}{\pi} \frac{8-3}{2(4-1)} \frac{6-3}{2(3-1)} \frac{4-3}{2(2-1)} \int_0^\infty \frac{1}{x^2 + 1} dx = \frac{5Z}{\pi 4} \arctan(x) \Big|_0^\infty = \frac{5Z}{\pi 4} \frac{\pi}{2} = \frac{5}{8} Z. \quad (140)$$

## B. Truncation near the singularities

In this section, we consider flattening the core orbital  $\varphi$  and nuclear potential  $V$  in the vicinity of the nucleus, and the Poisson kernel and Green function around their singularities. The radius at which we can flatten while maintaining acceptable relative error  $\epsilon$  indicates the scale at which an adaptive numerical method would need to refine. A larger radius means a coarser scale, and thus less computational cost. We conjecture that the core orbital is the extreme case, so this scale would suffice for general orbitals.

In the range  $2 \leq p \leq 6$  that we consider, the  $L^p$  norm on  $\varphi$  allows truncation at radii in the range from  $\epsilon^{2/5}$  to  $\epsilon^{2/3}$ . For  $\|\mathcal{W}_p[\phi\theta]\|_s$  the truncation radius is  $\epsilon^{us/(3u+2us-6s)}$  for  $3 < s \leq \infty$ , which is better for large  $u$  and small  $s$ . For  $u = 6$  all values of  $s$  give radius at least  $\epsilon^1$ , while for  $u = 4$  values  $3 < s \leq 6$  yield at least  $\epsilon^1$ . Thus these two objects do not present difficulties.

For  $\|V\phi\|_s$  the truncation radius is  $\epsilon^{us/(3u-3s-us)}$  for  $6/5 < s < 3u/(3+u)$ , which is better for small  $s$  and large  $u$ . The truncation radius for  $\mathcal{F}$ , which depends on the  $s$  chosen for  $\|V\phi\|_s$ , is  $\epsilon^{us/(2us+3s-3u)}$ , which is better for large  $s$  and small  $u$ . Thus  $V\phi$  and  $\mathcal{F}$  compete with each other. The product of these truncation radii is at most  $\epsilon^4$  independent of  $u$ , which is achieved by selecting  $s = 2u/(u+2)$  and results in both individual radii  $\epsilon^2$  independent of  $u$ . Therefore, we recommend choosing  $s = 2u/(u+2)$ .

For  $|\langle V, \phi\theta \rangle|$  the truncation radius is  $\epsilon^{u/(2u-6)}$ , which is better for large  $u$ . Choosing  $u = 6$  yields  $\epsilon^1$  and  $u = 4$  yields  $\epsilon^2$ . Thus this is the only term that is significantly worse for  $u = 4$  than for  $u = 6$ . However, we are already using radius  $\epsilon^2$  for  $V\phi$  so using it for  $|\langle V, \phi\theta \rangle|$  does not impose much additional burden. In particular, we can compute  $|\langle V, \phi\theta \rangle|$  as  $|\langle V\phi, \theta \rangle|$  and use the  $V\phi$  that we already computed. Choosing  $u < 4$  would require radius smaller than  $\epsilon^2$ , so we recommend choosing  $4 \leq u \leq 6$ .

### 1. Flattening the core orbital

Consider the flattened core orbital

$$\tilde{\varphi}(\mathbf{r}) = \begin{cases} Z^{3/2} \pi^{-1/2} \exp(-Z\delta) & \text{for } \|\mathbf{r}\| \leq \delta \\ Z^{3/2} \pi^{-1/2} \exp(-Z\|\mathbf{r}\|) = \varphi(\mathbf{r}) & \text{for } \delta < \|\mathbf{r}\|. \end{cases} \quad (141)$$

The error function is given on the ball of radius  $\delta$  by

$$\begin{aligned}\varphi(\|\mathbf{r}\|) - \tilde{\varphi}(\|\mathbf{r}\|) &= Z^{3/2} \pi^{-1/2} (1 - Z\|\mathbf{r}\| + \mathcal{O}(Z^2\|\mathbf{r}\|^2)) - (1 - Z\delta + \mathcal{O}(Z^2\delta^2)) \\ &= Z^{5/2} \pi^{-1/2} (\delta - \|\mathbf{r}\|) (1 + \mathcal{O}(Z\delta)).\end{aligned}\quad (142)$$

We can then compute

$$\begin{aligned}\|\varphi - \tilde{\varphi}\|_p &= \left( 4\pi \int_0^\delta \frac{Z^{5p/2}}{\pi^{p/2}} (\delta - r)^p (1 + \mathcal{O}(Z\delta))^p r^2 dr \right)^{1/p} \\ &= \frac{Z^{5/2}}{\pi^{1/2}} (1 + \mathcal{O}(Z\delta)) \left( 4\pi \int_0^\delta (\delta - r)^p r^2 dr \right)^{1/p} \\ &= \frac{Z^{5/2}}{\pi^{1/2}} (1 + \mathcal{O}(Z\delta)) \left( \frac{8\pi \delta^{p+3}}{(p+1)(p+2)(p+3)} \right)^{1/p}.\end{aligned}\quad (143)$$

Compared to the exact value from (128), we have relative error

$$\|\varphi - \tilde{\varphi}\|_p / \|\varphi\|_p = (1 + \mathcal{O}(Z\delta)) \left( \frac{p^3}{(p+1)(p+2)(p+3)} \right)^{1/p} (Z\delta)^{(p+3)/p} \quad (144)$$

so to obtain relative error  $\epsilon$  we need

$$(Z\delta)^{(p+3)/p} \sim \epsilon \Leftrightarrow Z\delta \sim \epsilon^{p/(p+3)}. \quad (145)$$

For  $p = 2$  we have  $Z\delta \sim \epsilon^{2/5}$ . For larger  $p$  the exponent  $p/(p+3)$  gets larger and so the radius  $\epsilon^{p/(p+3)}$  gets smaller and the condition (145) becomes more and more restrictive. For  $p = 6$  we have  $Z\delta \sim \epsilon^{2/3}$  and as  $p \rightarrow \infty$  we have  $Z\delta \sim \epsilon$ .

## 2. Truncating the nuclear potential

The potential  $V(\mathbf{r}) = -Z/\|\mathbf{r}\|$  is infinite at  $\|\mathbf{r}\| = 0$ , so any numerical method will have to cut it off at some radius. We consider the modified potential

$$\tilde{V}(\mathbf{r}) = \begin{cases} \frac{-Z}{\delta} & \text{for } \|\mathbf{r}\| \leq \delta \\ \frac{-Z}{\|\mathbf{r}\|} = V(\mathbf{r}) & \text{for } \delta < \|\mathbf{r}\| \end{cases}, \quad (146)$$

and will determine the dependence of the resulting errors on  $\delta$ .

The  $L^p$  norm of the error in the kernel is

$$\left\| \left( \frac{Z}{\|\mathbf{r}\|} - \frac{Z}{\delta} \right) \right\|_{\|\mathbf{r}\| \leq \delta} \Bigg|_p = \left( 4\pi Z^p \int_0^\delta (r^{-1} - \delta^{-1})^p r^2 dr \right)^{1/p} = \left( 4\pi \int_0^1 (t^{-1} - 1)^p t^2 dt \right)^{1/p} Z\delta^{(3-p)/p}, \quad (147)$$

so the error relative to  $\|V_{\text{near}}\|_p$  from (96) is

$$\|V - \tilde{V}\|_p / \|V_{\text{near}}\|_p = \left( (3-p) \int_0^1 (t^{-1} - 1)^p t^2 dt \right)^{1/p} \left( \frac{C_v \delta}{Z} \right)^{(3-p)/p}, \quad (148)$$

and the scaling is

$$\left( \frac{C_v \delta}{Z} \right)^{(3-p)/p} \sim \epsilon \Leftrightarrow \frac{C_v \delta}{Z} \sim \epsilon^{p/(3-p)}. \quad (149)$$

We note that if  $C_v$  is chosen as in (102) and the values for the core orbital from (130) inserted, then

$$C_v \delta / Z = Z\delta \pi^{2/3} (u-2)^{1/3} 2^{(2u+4)/(3u-6)} (u-3)^{2/(3u-6)} u^{-(u+6)/(3u-6)}, \quad (150)$$

which is proportional to  $Z\delta$ .

The bound on  $\|V_{\text{near}}\|_p$  is used in the bounds on  $|\langle V, \phi\theta \rangle|$  and  $\|V\phi\|_s$ . These bounds can be considered independently and do not need to use the same truncation radius. For  $|\langle V, \phi\theta \rangle|$ , in (101)

we use  $\|V_{\text{near}}\|_{u/(u-2)}$ , which results in scaling  $\epsilon^{u/(2u-6)}$ . Thus  $u = 6$  yields  $\epsilon^1$ ,  $u = 5$  yields  $\epsilon^{5/4}$ , and  $u = 4$  yields  $\epsilon^2$ . For  $\|V\phi\|_s$  in (105) we use  $\|V_{\text{near}}\|_{us/(u-s)}$  for  $6/5 < s < 3u/(3+u)$ , which results in scaling  $\epsilon^{us/(3u-3s-us)}$ . The exponent is reduced by making  $s$  smaller and  $u$  larger. For  $u = 6$  choosing  $s = 3/2$  yields  $\epsilon^2$ ,  $s = 5/4$  yields  $\epsilon^{10/9}$ , and  $s \rightarrow 6/5^+$  yields  $\epsilon^1$ . For  $u = 4$  choosing  $s = 4/3$  yields  $\epsilon^2$ ,  $s = 5/4$  yields  $\epsilon^{20/13}$ , and  $s \rightarrow 6/5^+$  yields  $\epsilon^{4/3}$ .

### 3. Truncating the poisson kernel

The kernel  $1/\|\mathbf{r}\|$  is infinite at  $\|\mathbf{r}\| = 0$ , so any numerical method will have to cut it off. We will modify the kernel by replacing  $1/\|\mathbf{r}\|$  with  $1/\delta$  when  $\|\mathbf{r}\| < \delta$ .

The  $L^p$  norm of the error in the kernel can be directly computed (as in (147)) as

$$\left\| \left( \frac{1}{\|\mathbf{r}\|} - \frac{1}{\delta} \right) \right\|_{\|\mathbf{r}\| \leq \delta} \Bigg|_p = \left( 4\pi \int_0^\delta (r^{-1} - \delta^{-1})^p r^2 dr \right)^{1/p} = \left( 4\pi \int_0^1 (t^{-1} - 1)^p t^2 dt \right)^{1/p} \delta^{(3-p)/p}, \quad (151)$$

so the error relative to  $\|\mathcal{W}_{\mathcal{P}}[\cdot]_{\text{near}}\|_p$  from (109) is

$$\left\| \left( \frac{1}{\|\mathbf{r}\|} - \frac{1}{\delta} \right) \right\|_{\|\mathbf{r}\| \leq \delta} \Bigg|_p / \|\mathcal{W}_{\mathcal{P}}[\cdot]_{\text{near}}\|_p = \left( (3-p) \int_0^1 (t^{-1} - 1)^p t^2 dt \right)^{1/p} \left( \frac{\delta}{C_w} \right)^{(3-p)/p}, \quad (152)$$

and the scaling is

$$\left( \frac{\delta}{C_w} \right)^{(3-p)/p} \sim \epsilon \Leftrightarrow \frac{\delta}{C_w} \sim \epsilon^{p/(3-p)}. \quad (153)$$

We note that if  $C_w$  is chosen as in (113) and the values for the core orbital from (130) inserted, then

$$\frac{\delta}{C_w} = \frac{Z\delta}{\pi^{1/3}} \left( \left( \frac{4\pi}{s-3} \right)^{1/s} \left( \frac{4\pi(u+us-2s)}{3u+2us-6s} \right)^{-(u+us-2s)/(us)} \frac{(s-3)u}{(3u+2us-6s)} \right)^{-u/(3u-6)} \left( \frac{2}{u} \right)^{2/(u-2)}, \quad (154)$$

which is proportional to  $Z\delta$ .

For  $\|\mathcal{W}_{\mathcal{P}}[\phi\theta]\|_s$ , in (112) we used  $\|\mathcal{W}_{\mathcal{P}}[\cdot]_{\text{near}}\|_{us/(u+us-2s)}$ , which results in scaling  $\epsilon^{us/(3u+2us-6s)}$ . For  $u = 6$ , choosing  $s = \infty$  yields  $\epsilon^1$ ,  $s = 6$  yields  $\epsilon^{2/3}$ ,  $s = 4$  yields  $\epsilon^{4/7}$ , and  $s \rightarrow 3^+$  yields  $\epsilon^{1/2}$ . For  $u = 4$ , choosing  $s = \infty$  yields  $\epsilon^2$ ,  $s = 6$  yields  $\epsilon^1$ ,  $s = 4$  yields  $\epsilon^{4/5}$ , and  $s \rightarrow 3^+$  yields  $\epsilon^{2/3}$ .

### 4. Truncating the Green function

As we saw in Sec. II C 4, the accuracy requirements on  $\mathcal{F}$  are equivalent to accuracy requirements on the Green function  $\mathcal{G}_\mu$  for the  $N = 1$  case. For  $N = 1$ , one can compute directly that the kernel of  $\mathcal{G}_\mu$  is

$$\frac{1}{2\pi} \frac{\exp(-\sqrt{-2\mu}\|\mathbf{r}\|)}{\|\mathbf{r}\|} \quad (155)$$

and using (56) that

$$\begin{aligned} \left\| \frac{1}{2\pi} \frac{\exp(-\sqrt{-2\mu}\|\mathbf{r}\|)}{\|\mathbf{r}\|} \right\|_p &= \left( 4\pi \int_0^\infty \left( \frac{1}{2\pi} \frac{\exp(-\sqrt{-2\mu}r)}{r} \right)^p r^2 dr \right)^{1/p} \\ &= \frac{1}{2\pi} \left( 4\pi \Gamma(3-p) (p\sqrt{-2\mu})^{p-3} \right)^{1/p}. \end{aligned} \quad (156)$$

Since the kernel (155) is infinite at  $\|\mathbf{r}\| = 0$ , we modify it by replacing it by  $\exp(-\sqrt{-2\mu}\delta)/(2\pi\delta)$  when  $\|\mathbf{r}\| < \delta$ . For  $1 \leq p < 3$ , the  $L^p$  norm of the error is

$$\begin{aligned} & \left( 4\pi \int_0^\delta \left( \frac{1}{2\pi} \frac{\exp(-\sqrt{-2\mu}r)}{r} - \frac{1}{2\pi} \frac{\exp(-\sqrt{-2\mu}\delta)}{\delta} \right)^p r^2 dr \right)^{1/p} \\ & \leq \frac{1}{2\pi\delta} \left( 4\pi \int_0^1 \left( \frac{\exp(-\sqrt{-2\mu}\delta s)}{s} \right)^p \delta^3 s^2 ds \right)^{1/p} \\ & \leq \frac{1}{2\pi\delta} \left( 4\pi \int_0^1 \left( \frac{1}{s} \right)^p \delta^3 s^2 ds \right)^{1/p} = 2^{-1+2/p} \pi^{-1+1/p} \delta^{-1+3/p} (3-p)^{-1/p}. \end{aligned} \quad (157)$$

Dividing by the exact value (156) and inserting  $\mu = -Z^2/2$  from (127) for the core orbital, we have relative error

$$(\delta Z)^{(3-p)/p} (3-p)^{-1/p} (\Gamma(3-p))^{-1/p} p^{(3-p)/p}. \quad (158)$$

Thus to have relative error less than  $\epsilon$  we need

$$\delta Z < \epsilon^{p/(3-p)} (3-p)^{1/(3-p)} p^{-1} \Gamma(3-p)^{1/(3-p)} \quad \text{so} \quad \delta Z \sim \epsilon^{p/(3-p)}, \quad (159)$$

which is better for smaller  $p$ .

The operator  $\mathcal{F}$  is used in several places and will use several different  $p$ . The largest  $p$  occurs in the sequence of operations  $\phi \rightarrow V\phi \rightarrow \mathcal{F}V\phi$  with spaces  $L^{[2,u]} \rightarrow L^s \rightarrow L^{[2,u]}$ . In Sec. IV B 2, we saw that  $\|V\phi\|_s$  allows truncation of the singularity scaling as  $\delta Z \sim \epsilon^{us/(3u-3s-us)}$ . For the map  $\mathcal{F} : L^s \rightarrow L^u$  we have  $p = us/(us + s - u)$  so (159) becomes

$$\delta Z \sim \epsilon^{us/(2us+3s-3u)}. \quad (160)$$

We thus see that the choices of  $u$  and  $s$  affect the scaling of two different objects. Consider the product of these two truncation scalings, which yields exponent

$$\frac{u^2 s^2}{(3u - 3s - us)(2us + 3s - 3u)}. \quad (161)$$

Explicitly minimizing this function, we find it has a minimum along the line

$$us + 2s - 2u = 0 \quad \Leftrightarrow \quad s = \frac{2u}{u+2}, \quad (162)$$

and there has value 4, independent of  $u$ . Inserting the optimal relationship (162) into the two truncation scalings, we find both reduce to  $\epsilon^2$ , independent of  $u$ .

### C. Comparison of bounds

In this section, we test our bounds from Sec. III using the core orbital. Our goal is to determine the efficiency of the bounds to help us decide on which spaces to use for the intermediate steps.

In Sec. IV B, we concluded that one should use  $L^2 \cap L^u$  with  $4 \leq u \leq 6$  for the inputs. For  $\phi\theta$  and  $\tilde{\phi}\tilde{\theta}$ , using the extremal spaces  $L^1 \cap L^{u/2}$  does not appear to have any disadvantages, so we recommend it. For  $\tilde{\phi}\mathcal{W}_p[\phi\theta]$ , in Sec. IV C 3 in Figure 5 we show that using  $L^2$  gives nearly optimal output for  $\mathcal{F}\tilde{\phi}\mathcal{W}_p[\phi\theta]$ , so we recommend it. For  $\mathcal{W}_p[\phi\theta]$ , in Sec. IV C 3 in Figure 6 we show that  $L^5$  is nearly optimal, but all spaces from  $L^4$  to  $L^\infty$  are comparable. In Sec. IV B 3, we showed that the best scaling is  $\epsilon^{1/2}$  as  $s \rightarrow 3^+$ , but that even  $s = \infty$  gives acceptable scaling  $\epsilon$ . On balance we recommend  $L^4$ , which gives scaling  $\epsilon^{4/7}$ . For  $V\phi$ , in Sec. IV B 4 we showed that the best compromise scaling of  $\epsilon^2$  is obtained by taking  $s = 2u/(u+2) = 3/2$ .

None of these considerations determine which  $u \in [4, 6]$  we should choose. In fact, all our tests below show that  $u = 4$  and  $u = 6$  give comparable results. Thus, on the general principle that weaker function spaces are easier for a numerical method to accomplish, we recommend choosing  $u = 4$ . These recommendations are summarized in the diagram (27).

TABLE I. Sharpness factors for various bounds.

Quantity	Exact Value	Bound	Using Value	Sharpness Factor	
				Assuming $L^{[2,4]}$	Assuming $L^{[2,6]}$
$ \langle V, \varphi^2 \rangle $	(132)	(103)	(130)	$3/2 = 1.5$	$2 \cdot 3^{1/6} \approx 2.40$
$\ V\varphi\ _{4/3}$	(134)	(107)	(128)	$2^{3/4} 3^{-1/4} \Gamma(5/3)^{-3/4} \approx 1.38$	...
$\ V\varphi\ _{3/2}$	(134)	(107)	(128)	...	$(3/2)^{2/3} \Gamma(3/2)^{-2/3} \approx 1.42$
$\ \mathcal{W}_P[\varphi^2]\ _\infty$	(133)	(117)	(130)	$3/2 = 1.5$	$2^2 3^{-5/6} \approx 1.61$
$\langle \varphi^2, \mathcal{W}_P[\varphi^2] \rangle$	(140)	(119), (117)	(130)	$12/5 = 2.4$	$2^5 3^{-5/6} 5^{-1} \approx 2.57$

## 1. Sharpness

An inequality is said to be sharp if equality is attained for some inputs. For an inequality of the form  $A(f) \leq B(f)$ , the ratio  $B(f)/A(f)$  is the sharpness factor for that  $f$ , and  $C = \min_f B(f)/A(f) \geq 1$  is the sharpness factor for the inequality. If  $C$  is known, then the sharp inequality  $A(f) \leq B(f)/C$  could be used. If  $C$  is not known but for trial  $f$  the ratio  $B(f)/A(f)$  is large, then one is stuck using a potentially inefficient bound. In particular, one may need to make  $\|f\|$  unreasonably small in order to be assured that  $A(f)$  is acceptably small.

We now check some of the bounds in Sec. III by using the exact values available for the core orbital from Sec. IV A. Due to lack of exact values, we are unable to check  $\|\mathcal{W}_P[\varphi^2]\|_s$  for  $s < \infty$ ,  $\|\varphi \mathcal{W}_P[\varphi^2]\|_t$ , or any quantities involving  $\mathcal{F}$ . We organize the results in Table I. We find that the sharpness factors are all less than 3.

## 2. Intermediate objects

In this section, we discuss our bounds for  $\|\mathcal{W}_P[\varphi^2]\|_s$  with  $s < \infty$  and  $\|\varphi \mathcal{W}_P[\varphi^2]\|_t$ , for which we have no exact formulas, and for  $|\langle \varphi^2, \mathcal{W}_P[\varphi^2] \rangle|$  when using  $\|\mathcal{W}_P[\varphi^2]\|_s$ .

Our bound on  $\|\mathcal{W}_P[\phi\theta]\|_s$  is given by (114). Inserting the exact values (128) for the core orbital and normalizing by the exact value  $\|\mathcal{W}_P[\varphi^2]\|_\infty = Z$ , we obtain a bound for  $\|\mathcal{W}_P[\varphi^2]\|_s/Z$  as a function of  $s$  and  $u$ . We plot the result in Figure 2 for  $u = 4$  and  $u = 6$ . We observe that there is little difference between  $u = 4$  and  $u = 6$  and that although the bound becomes untenable as  $s \rightarrow 3^+$ , at  $s = 3.2$  the inflation is less than 4.

The value of  $\|\mathcal{W}_P[\phi\theta]\|_s$  is used in the bound (119) for  $|\langle \tilde{\phi}\tilde{\theta}, \mathcal{W}_P[\phi\theta] \rangle|$ . Since we know the exact value from (140), we can compute the sharpness factor as a function of  $u$  and the intermediate

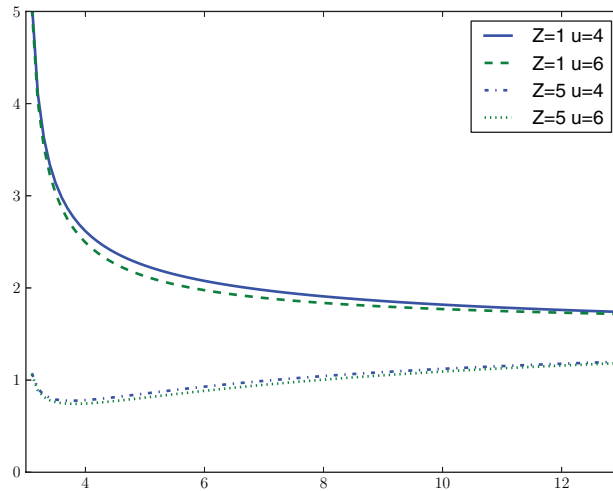


FIG. 2. The bound on  $\|\mathcal{W}_P[\varphi^2]\|_s/Z$  (vertical axis) as a function of  $s$  (horizontal axis,  $[3.1, 13]$ ) using the bound (114) and assuming only  $\varphi \in L^{[2,u]}$ . The bound becomes infinite at  $s = 3$ .

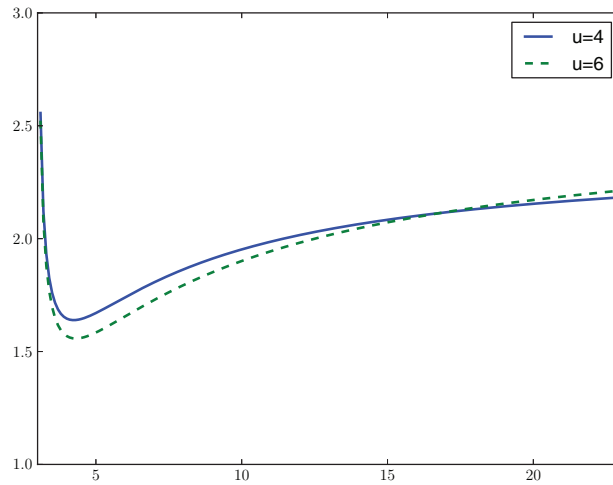


FIG. 3. The sharpness bound on  $|\langle \varphi^2, \mathcal{W}_{\mathcal{P}}[\varphi^2] \rangle / (5/8Z)|$  (vertical axis) as a function of the  $s$  (horizontal axis,  $[3.1, 23]$ ) used for  $\|\mathcal{W}_{\mathcal{P}}[\varphi^2]\|_s$ , which assumes only  $\varphi \in L^{[2, 6]}$ . The bounds become infinite at  $s = 3$  and go to values less than 3 as  $s \rightarrow \infty$ .

$s$  used. We plot the result in Figure 3. We observe that the values for  $3.1 < s < \infty$  are better than the value in Table I, which used  $s = \infty$ .

Our bound on  $\|\tilde{\phi}\mathcal{W}_{\mathcal{P}}[\phi\theta]\|_t$  is given by (118) for  $6/5 < t \leq u$  and depends on an intermediate parameter  $s$ , which determines which norm is used for  $\mathcal{W}_{\mathcal{P}}[\phi\theta]$ , as well as the initial  $u$ . We plot the result for the core orbital in Figure 4. We observe that  $u = 4$  and  $u = 6$  give similar results and that different values of  $s$  are needed for different values of  $t$ .

### 3. Minimal output size

As discussed in Sec. IV B, we recommend taking  $V\phi \in L^{2u/(u+2)}$ . The bound on  $\|\mathcal{F}V\phi\|_q$  is obtained by multiplying (107) with  $s = 2u/(u + 2)$  by (67) with  $p = 2uq/(uq + 2u - 2q)$ . Inserting the exact values (128) and (127) for the core orbital and normalizing by  $\|\varphi\|_q$ , we obtain a bound for  $\|\mathcal{F}V\phi\|_q / \|\varphi\|_q$  as a function of  $u$ . The resulting bound is independent of  $Z$ . Since we are only interested in  $q = 2$  and  $q = u$ , and are only testing  $u = 4$  and  $u = 6$ , there are only four values to

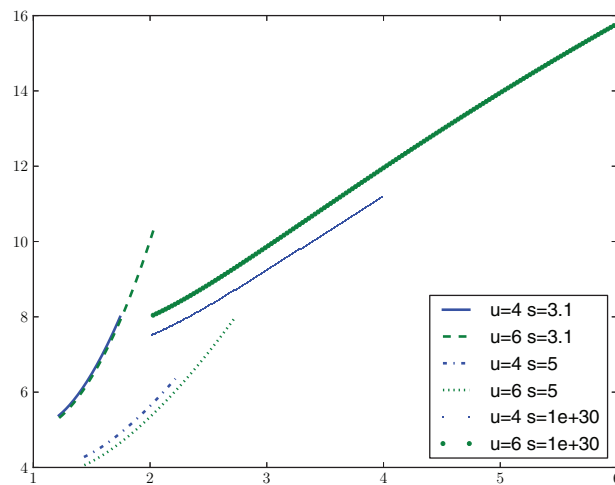


FIG. 4. The bound on  $\|\varphi\mathcal{W}_{\mathcal{P}}[\varphi^2]\|_t$  (vertical axis) as a function of  $t$  (horizontal axis) using  $Z = 5$  and three values for  $s$  in (118).

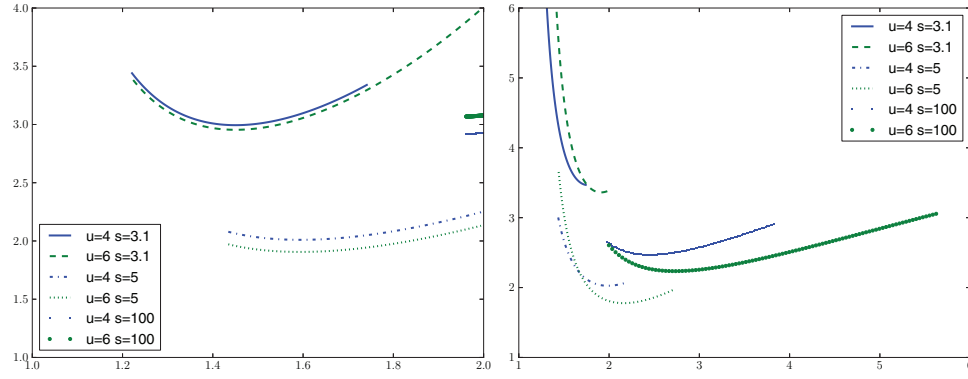


FIG. 5. The bound on  $Z\|\mathcal{F}\varphi\mathcal{W}_P[\varphi^2]\|_q/\|\varphi\|_q$  (vertical axis) for  $q = 2$  (left plot) and  $q = u$  (right plot) as a function of the  $t$  (horizontal axis) used for  $\|\varphi\mathcal{W}_P[\varphi^2]\|_t$  for a selection of  $s$  used for  $\|\mathcal{W}_P[\varphi^2]\|_s$ .

compute. For  $u = 4$  and  $q = 2$  we have 2.69, for  $u = 4$  and  $q = 4$  we have 4.85, for  $u = 6$  and  $q = 2$  we have 2.76, and for  $u = 6$  and  $q = 6$  we have 4.36.

Our bound on  $\|\mathcal{F}\tilde{\phi}\mathcal{W}_P[\phi\theta]\|_q$  is obtained by multiplying (67) using  $p = (1 + 1/q - 1/t)^{-1}$  by (118) for some  $6/5 < t \leq u$ , which depends on a  $s$ , which determines which norm is used for  $\mathcal{W}_P[\phi\theta]$  in (112). Assembling these together and inserting values for the core orbital, we obtain an incomprehensible formula depending on  $u$ ,  $s$ ,  $t$ , and  $q$ . We do, however, note  $Z$ -dependence of  $Z^{-1}$ . To study the behavior with respect to  $t$  and  $s$ , we therefore normalize by  $Z^{-1}$  and consider  $Z\|\mathcal{F}\varphi\mathcal{W}_P[\varphi^2]\|_q/\|\varphi\|_q$ . In Figure 5, we plot the bounds for  $q = 2$  and  $q = u$  using  $u = 4$  and  $u = 6$ . For  $q = 2$  we observe that  $t = 1.5$  appears optimal, but  $t = 2$  is only slightly worse. For  $q = u$  the optimum is near  $t = 2$  and smaller  $t$  are significantly worse. Thus  $t = 2$  appears to be the best choice. We observe in both cases that the best  $s$  are around  $s = 5$ . To test this, we next fix  $t = 2$  and plot the bounds as a function of  $s$  in Figure 6. The optimum appears to be just less than 5.

Our other two outputs consist of  $\mathcal{F}\tilde{\phi}$  or  $\mathcal{F}\tilde{\phi}$  times a scalar. Using the  $L^2$  norm of  $\varphi$ , we can apply (67) with  $p = 2q/(2 + q)$  to obtain the bound

$$\frac{\|\mathcal{F}\varphi\|_q}{\|\varphi\|_q} \leq Z^{-2} \Gamma\left(\frac{6+q}{4q}\right) 2^{-(5q+6)/(4q)} \pi^{(2-q)/(4q)} (2+q)^{3(2+q)/(4q)} q^{(6-3q)/(4q)}. \quad (163)$$

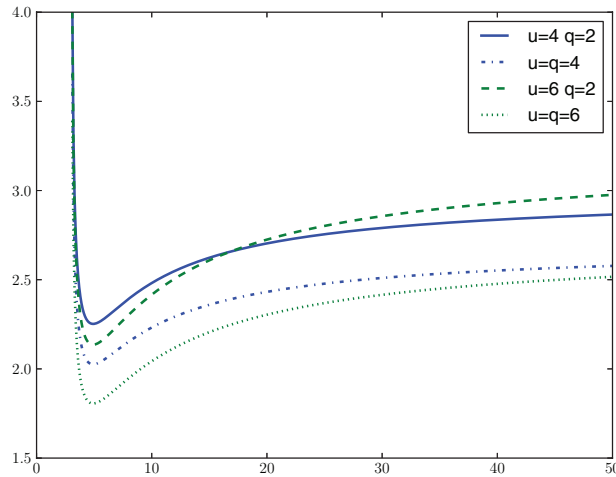


FIG. 6. The bound on  $Z\|\mathcal{F}\varphi\mathcal{W}_P[\varphi^2]\|_q/\|\varphi\|_q$  (vertical axis) for  $q = 2$  and  $q = u$  as a function of the  $s$  (horizontal axis;  $[3.1, 50]$ ) used for  $\|\mathcal{W}_P[\varphi^2]\|_s$ .

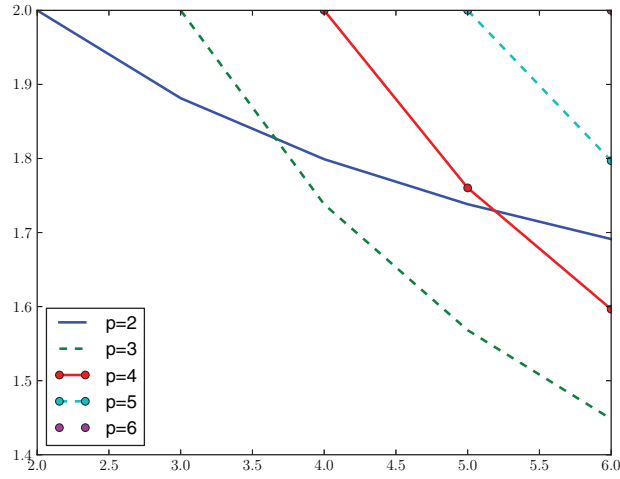


FIG. 7. The bound on  $Z^2 \|\mathcal{F}\varphi\|_q / \|\varphi\|_q$  (vertical axis) as a function of  $q$  (horizontal axis) for a selection of  $p$  used for  $\|\varphi\|_p$ .

Alternatively, we can use the  $L^q$  norm of  $\varphi$  and apply (67) with  $p = 1$  to obtain simply  $2Z^{-2}$ , independent of  $q$ . In Figure 7, we illustrate the bounds on  $Z^2 \|\mathcal{F}\varphi\|_q / \|\varphi\|_q$  for a selection of  $L^p$  assumptions on  $\varphi$ . We observe that although  $p = 3$  gives a better bound for  $q > 3$ , the bound using  $p = 2$  is quite similar.

## V. IMPLEMENTATION AND TESTING

### A. Bound collection

In this section, we collect the bounds used for our final choice of function spaces (27). These bounds are obtained by inserting particular values into bounds obtained elsewhere in the paper.

From (85) and (93) we have

$$\|\phi\theta\|_1 \leq \|\phi\|_2 \|\theta\|_2 \quad \text{and} \quad (164)$$

$$\|\phi\theta\|_2 \leq \|\phi\|_4 \|\theta\|_4. \quad (165)$$

From (103) and (107) we have

$$|\langle V, \phi\theta \rangle| \leq Z_{\text{total}} 3\pi^{1/3} (\|\phi\theta\|_1 \|\phi\theta\|_2^2)^{1/3} \leq 4.40 Z_{\text{total}} ((164) \times (165)^2)^{1/3} \quad \text{and} \quad (166)$$

$$\|V\phi\|_{4/3} \leq Z_{\text{total}} 3\pi^{1/3} (\|\phi\|_2^2 \|\phi\|_4)^{1/3} \leq 4.40 Z_{\text{total}} (\|\phi\|_2^2 \|\phi\|_4)^{1/3}. \quad (167)$$

From (114), (118), and (119) we have

$$\|\mathcal{W}_{\mathcal{P}}[\phi\theta]\|_4 \leq 2^{5/3} 3^{9/8} 5^{-23/24} \pi^{1/3} (\|\phi\theta\|_1^5 \|\phi\theta\|_2)^{1/6} \leq 3.43 ((164)^5 \times (165))^{1/6}, \quad (168)$$

$$\|\tilde{\phi}\mathcal{W}_{\mathcal{P}}[\phi\theta]\|_2 \leq \|\tilde{\phi}\|_4 \|\mathcal{W}_{\mathcal{P}}[\phi\theta]\|_4 \leq \|\tilde{\phi}\|_4 \times (168), \quad (169)$$

$$|\langle \tilde{\phi}\tilde{\theta}, \mathcal{W}_{\mathcal{P}}[\phi\theta] \rangle| \leq \|\tilde{\phi}\tilde{\theta}\|_{4/3} \|\mathcal{W}_{\mathcal{P}}[\phi\theta]\|_4 \leq (\|\tilde{\phi}\tilde{\theta}\|_1 \|\tilde{\phi}\tilde{\theta}\|_2)^{1/2} \times (168) \leq ((164) \times (165))^{1/2} \times (168). \quad (170)$$

From (67) we obtain the operator bounds  $\mathcal{F} : L^q \rightarrow L^s$  of

$$L^q \rightarrow L^q : \|\mathcal{F}\|_1 \sim (-\mu)^{-1}, \quad (171)$$

$$L^2 \rightarrow L^4 \text{ and } L^{4/3} \rightarrow L^2 : \|\mathcal{F}\|_{4/3} \sim \Gamma(5/8)2^{-21/8}3^{9/8}\pi^{-3/8}(-\mu)^{-5/8} \leq 0.521(-\mu)^{-5/8}, \quad (172)$$

$$L^{4/3} \rightarrow L^4 : \|\mathcal{F}\|_2 \sim \Gamma(1/4)2^{-3/2}\pi^{-3/4}(-\mu)^{-1/4} \leq 0.544(-\mu)^{-1/4}. \quad (173)$$

Assembling these together, we have

$$\|\mathcal{F}\tilde{\phi}\|_2 \leq \|\mathcal{F}\|_1 \|\tilde{\phi}\|_2 = (171) \times \|\tilde{\phi}\|_2, \quad (174)$$

$$\|\mathcal{F}\tilde{\phi}\|_4 \leq \|\mathcal{F}\|_{4/3} \|\tilde{\phi}\|_2 = (172) \times \|\tilde{\phi}\|_2, \quad (175)$$

$$\|\mathcal{F}\tilde{\phi} \langle V, \phi\theta \rangle\|_2 \leq \|\mathcal{F}\tilde{\phi}\|_2 |\langle V, \phi\theta \rangle| \leq (174) \times (166), \quad (176)$$

$$\|\mathcal{F}\tilde{\phi} \langle V, \phi\theta \rangle\|_4 \leq \|\mathcal{F}\tilde{\phi}\|_4 |\langle V, \phi\theta \rangle| \leq (175) \times (166), \quad (177)$$

$$\|\mathcal{F}\tilde{\phi} \langle \tilde{\phi}\tilde{\theta}, \mathcal{W}_{\mathcal{P}}[\phi\theta] \rangle\|_2 \leq \|\mathcal{F}\tilde{\phi}\|_2 \|\langle \tilde{\phi}\tilde{\theta}, \mathcal{W}_{\mathcal{P}}[\phi\theta] \rangle\| \leq (174) \times (170), \quad (178)$$

$$\|\mathcal{F}\tilde{\phi} \langle \tilde{\phi}\tilde{\theta}, \mathcal{W}_{\mathcal{P}}[\phi\theta] \rangle\|_4 \leq \|\mathcal{F}\tilde{\phi}\|_4 \|\langle \tilde{\phi}\tilde{\theta}, \mathcal{W}_{\mathcal{P}}[\phi\theta] \rangle\| \leq (175) \times (170), \quad (179)$$

$$\|\mathcal{F}\tilde{\phi}\mathcal{W}_{\mathcal{P}}[\phi\theta]\|_2 \leq \|\mathcal{F}\|_1 \|\tilde{\phi}\mathcal{W}_{\mathcal{P}}[\phi\theta]\|_2 \leq (171) \times (169), \quad (180)$$

$$\|\mathcal{F}\tilde{\phi}\mathcal{W}_{\mathcal{P}}[\phi\theta]\|_4 \leq \|\mathcal{F}\|_{4/3} \|\tilde{\phi}\mathcal{W}_{\mathcal{P}}[\phi\theta]\|_2 \leq (172) \times (169), \quad (181)$$

$$\|\mathcal{F}V\phi\|_2 \leq \|\mathcal{F}\|_{4/3} \|V\phi\|_{4/3} \leq (172) \times (167), \quad \text{and} \quad (182)$$

$$\|\mathcal{F}V\phi\|_4 \leq \|\mathcal{F}\|_2 \|V\phi\|_{4/3} \leq (173) \times (167). \quad (183)$$

## B. Truncation radius collection

In this section, we gather the truncation radii from Sec. IV B given our choices of spaces in (27). These radii are obtained by inserting particular values into the formulas.

For  $\varphi$ , we chose to use  $p = 2$  and  $p = 4$ . Assuming  $\mathcal{O}(Z\delta) < 1$ , from (144) and (145) we have the sufficient condition

$$\delta < Z^{-1} \left(\frac{\epsilon}{2}\right)^{p/(p+3)} \left(\frac{(p+1)(p+2)(p+3)}{p^3}\right)^{1/(p+3)}. \quad (184)$$

Inserting  $p = 4$  yields  $\delta < 0.797 \epsilon^{4/7}/Z$ , which is more restrictive than the  $p = 2$  radius.

For  $V$  we chose  $u = 4$  so from (150) we obtain

$$C_v = Z^2 2^{-1} \pi^{2/3} \quad \text{and} \quad C_v \delta / Z = Z \delta 2^{-1} \pi^{2/3}. \quad (185)$$

For  $|\langle V, \phi\theta \rangle|$  we have  $p = 2$  in (148) and obtain  $(Z\delta)^{1/2} 2^{-1/2} 3^{-1} \pi^{1/3} < 0.346 (Z\delta)^{1/2}$ ; thus to obtain error less than  $\epsilon$ , it is sufficient to have  $\delta < 8.39 \epsilon^2/Z$ . For  $\|V\phi\|_{4/3}$  we also have  $p = 2$  in (148) and so obtain the same radius.

For  $\mathcal{W}_{\mathcal{P}}[\cdot]$ , we chose  $u = 4$  and  $s = 4$ , so from (154) we obtain

$$C_w = Z^{-1} 2^{1/3} 3^{-1/2} 5^{-1/6} \quad \text{and} \quad \frac{\delta}{C_w} = Z \delta 2^{-1/3} 3^{1/2} 5^{1/6}. \quad (186)$$

We have  $p = us/(u + us - 2s) = 4/3$  in (152) and obtain

$$(Z\delta)^{5/4} 2^{-5/12} 3^{-1/8} 5^{23/24} \left(\int_0^1 (1-t)^{4/3} t^{2/3} dt\right)^{3/4} < (Z\delta)^{5/4} 2^{11/12} 3^{-17/8} 5^{23/24} < 0.855 (Z\delta)^{5/4}; \quad (187)$$

thus to obtain error less than  $\epsilon$ , it is sufficient to have  $\delta < 1.16 \epsilon^{4/5}/Z$ . From the splitting (112) with  $C_w$  from (186) we have that  $\mathcal{W}_P[\cdot]_{\text{far}} : L^1 \rightarrow L^4$  is bounded by

$$\left\| \frac{1}{\|\mathbf{r}\|} \right\|_{C_w < \|\mathbf{r}\|}_4 = Z^{1/4} 2^{5/12} 3^{1/8} 5^{1/24} \pi^{1/4} < 2.19 Z^{1/4} \quad (188)$$

and  $\mathcal{W}_P[\cdot]_{\text{near}} : L^2 \rightarrow L^4$  is bounded by

$$\left\| \frac{1}{\|\mathbf{r}\|} \right\|_{\|\mathbf{r}\| \leq C_w}_{4/3} = Z^{-5/4} 2^{23/12} 3^{1/8} 5^{-23/24} \pi^{3/4} < 2.19 Z^{-5/4}. \quad (189)$$

For  $\mathcal{F}$ , the most strenuous operation is  $L^{4/3} \rightarrow L^4$ , which gives  $p = 2$  in (158) yielding  $2^{1/2}(\delta Z)^{1/2}$ ; thus to obtain error less than  $\epsilon$ , it is sufficient to have  $\delta < (1/2)\epsilon^2/Z$ . To enable the construction in Sec. II C 4 we also compute the error from truncating  $\mathcal{F}$  for  $D < r$  for the most restrictive case  $p = 1$ . The  $L^1$  norm of the error is

$$4\pi \int_D^\infty \frac{1}{2\pi} \frac{\exp(-\sqrt{-2\mu}r)}{r} r^2 dr = 2 \exp(-\sqrt{-2\mu}D) \frac{D(\sqrt{-2\mu}) + 1}{(\sqrt{-2\mu})^2}. \quad (190)$$

Dividing by the exact value (156) gives relative error  $\exp(-\sqrt{-2\mu}D)(D(\sqrt{-2\mu}) + 1)$  and inserting  $\mu = -Z^2/2$  from (127) for the core orbital yields  $\exp(-ZD)(ZD + 1)$ . We cannot get a closed form for the  $D$  that gives relative error less than  $\epsilon$ , but asymptotically it behaves as  $D \sim -\ln(\epsilon)/Z$ .

### C. Vector and matrix amplification

Since (22) is part of an iteration, we expect the sizes of the outputs to be similar to the sizes of the inputs. For the core orbital  $\varphi$ , using the spaces in (27) we find the bounds

$$\|\mathcal{F}\varphi\langle V, \varphi^2 \rangle\|_2 \leq 3 \|\varphi\|_2, \quad \|\mathcal{F}\varphi\langle V, \varphi^2 \rangle\|_4 \leq 2.70 \|\varphi\|_4, \quad (191)$$

$$\|\mathcal{F}V\varphi\|_2 \leq 2.70 \|\varphi\|_2, \quad \|\mathcal{F}V\varphi\|_4 \leq 4.86 \|\varphi\|_4, \quad (192)$$

$$\|\mathcal{F}\varphi\langle \varphi^2, \mathcal{W}_P[\varphi^2] \rangle\|_2 \leq 2.06 \|\varphi\|_2/Z, \quad \|\mathcal{F}\varphi\langle \varphi^2, \mathcal{W}_P[\varphi^2] \rangle\|_4 \leq 1.86 \|\varphi\|_4/Z, \quad (193)$$

$$\|\mathcal{F}\varphi\mathcal{W}_P[\varphi^2]\|_2 \leq 2.34 \|\varphi\|_2/Z, \quad \text{and} \quad \|\mathcal{F}\varphi\mathcal{W}_P[\varphi^2]\|_4 \leq 2.11 \|\varphi\|_4/Z, \quad (194)$$

where  $Z$  is the charge of the nucleus. The factors of  $Z$  are present because (22) does not account for linear combinations present in the construction of the functions in  $\mathbf{b}$  in (21). In this section, we discuss how these linear combinations amplify the expected sizes of the results of the sequences. We expect the result of (21) to have the same size as its inputs.

The elements in  $\Phi$  have  $\|\phi_i\|_2 = 1$ . The functions in  $\mathcal{F}\Phi$  do not have norm one, but their net norm was already accounted for when we collapsed all  $|\mathbb{E}^j| \mathcal{F}^j$  to a single  $\mathcal{F}$  in Sec. II C 3, so we can treat them as having norm one. The functions in  $\Theta$  were produced by a biorthogonalization process from  $\mathcal{F}\Phi$ , but the factor  $|\mathbb{E}| \approx |\mathbb{L}|$  incorporated into  $\mathcal{F}$  compensates for the net change in norm, so we can assume  $\|\theta_i\|_2 = 1$  as well. The elements in  $\Phi$  are orthogonal, since they were produced in a previous iteration and the matrix  $\mathbb{A}$  contains an orthogonal projection due to the antisymmetric inner product. By construction, the vector  $\mathbf{d}$  has  $\|\mathbf{d}\|_2 = 1$ , so we thus also have  $\|\Phi^* \mathbf{d}\|_2 = 1$  and so  $\Phi^* \mathbf{d}$  acts as a single  $\phi$  and does not amplify the magnitude. To collapse the remaining vector/matrix operations, we note the size of the vectors/matrices is  $N$ . Thus the linear combination in  $\Phi^* \Theta$  produces a function of size at most  $N$  times the size of the component  $\phi\theta$ .

In Table II, we organize our first estimates of the amplified sizes. We give the amplified estimate using  $N$  and then set  $N = Z$  to represent a neutral system. The terms coming from  $\mathcal{F}V\varphi$  and  $\mathcal{F}\varphi\mathcal{W}_P[\varphi^2]$  yield final size 1 as expected, but the other terms are too large by a factor of  $N = Z$ . We can identify the following possible causes for overestimation of the sizes:

TABLE II. Maximum amplification of terms due to linear combinations using core orbital sizes and  $-\mu \sim Z^2$ , neglecting constants.

Terms in (21)	Single core		Amplification	
	Term	Size	Raw	$N = Z$
$ \mathbb{E}  \mathcal{F} \Phi^* \mathbf{d} \int V \Phi^* \Theta d\gamma'$	$\ \mathcal{F} \varphi \langle V, \varphi^2 \rangle\ _q / \ \varphi\ _q$	1	$N$	$Z$
$ \mathbb{E}  \mathcal{F} (-1) \Phi^* \int V \Phi^* \mathbf{d} \Theta d\gamma'$				
$ \mathbb{E}  \mathcal{F} V \Phi^* \mathbf{d}$	$\ \mathcal{F} V \varphi\ _q / \ \varphi\ _q$	1	1	1
$ \mathbb{E}  \mathcal{F} \frac{1}{2} \Phi^* \mathbf{d} \int \Phi^* \Theta \mathcal{W}_P [\Phi^* \Theta] d\gamma'$	$\ \mathcal{F} \varphi \langle \varphi^2, \mathcal{W}_P [\varphi^2] \rangle\ _q / \ \varphi\ _q$	$Z^{-1}$	$N^2 Z^{-1}$	$Z$
$ \mathbb{E}  \mathcal{F} \frac{1}{2} \Phi^* \mathbf{d} \int \Phi^* \mathcal{W}_P [\Theta \Phi^*] \Theta d\gamma'$				
$ \mathbb{E}  \mathcal{F} \frac{1}{2} \Phi^* \int \Theta \mathcal{W}_P [\Phi^* \Theta] \Phi^* \mathbf{d} d\gamma'$				
$ \mathbb{E}  \mathcal{F} \frac{1}{2} \Phi^* \int \Theta \Phi^* \mathcal{W}_P [\Theta \Phi^* \mathbf{d}] d\gamma'$				
$ \mathbb{E}  \mathcal{F} \Phi^* \mathbf{d} \mathcal{W}_P [\Phi^* \Theta]$	$\ \mathcal{F} \varphi \mathcal{W}_P [\varphi^2]\ _q / \ \varphi\ _q$	$Z^{-1}$	$NZ^{-1}$	1
$ \mathbb{E}  \mathcal{F} (-1) \Phi^* \mathcal{W}_P [\Theta \Phi^* \mathbf{d}]$				

1. The core orbital is more concentrated around the nucleus than general orbitals, so the core orbital values  $\langle V, \varphi^2 \rangle = -Z^2$  and  $\|\mathcal{W}_P [\varphi^2]\|_\infty = Z$  that we used are too large for general orbitals.
2. We did not account for the biorthogonality property  $\langle \phi_i, \theta_j \rangle = 0$  for  $i \neq j$ , which leads to cancellations when integrating and thus makes functions such as  $\mathcal{W}_P [\phi_i \theta_j]$  small.

In Table III, we list those objects whose amplification we believe should be modified due to the reasons above in order to yield the expected sizes.

#### D. Antisymmetric inner products using the singular value decomposition (SVD)

The antisymmetric inner product formulas (7) and (8) require application of the matrix  $\mathbb{L}^{-1}$  and then multiplication by  $|\mathbb{L}|$ . In Ref. 3, we observed that when  $\mathbb{L}$  is singular the antisymmetric inner products still make sense, and can be computed using the SVD. Our experience since then indicated that formulas using the SVD are preferred even when  $\mathbb{L}$  is non-singular, since they are accurate even when  $\mathbb{L}$  is ill-conditioned. The SVD construction is no more costly than the original in the nonsingular case and allows small terms to be neglected in a controlled manner. In this section, we give the SVD-based formulas, which should be viewed as the method to implement the inverse-based formulas.

The singular value decomposition<sup>16</sup> of a  $N \times N$  matrix is

$$\mathbb{L} = \sum_{i=1}^N s_i \mathbf{u}_i \mathbf{v}_i^* = \mathbb{U} \mathbb{S} \mathbb{V}^*, \quad (195)$$

where the matrices  $\mathbb{U}$  and  $\mathbb{V}$  are unitary and the singular values  $\{s_i\}$  are non-negative and in descending order. The left singular vectors  $\{\mathbf{u}_i\}$  form an orthonormal set, as do the right singular

TABLE III. Modified amplification of terms.

Term	Maximum	Modified	Reason
$\int V \Phi^* \Theta d\gamma'$	$NZ^2$	$Z^2$	1
$\Phi^* \int V \Phi^* \mathbf{d} \Theta d\gamma'$	$NZ^2$	$Z^2$	1
$\mathcal{W}_P [\Phi^* \Theta]$	$NZ$	$Z$	1
$\int \Phi^* \mathcal{W}_P [\Theta \Phi^*] \Theta d\gamma'$	$N^2 Z$	$NZ$	2 for off-diagonals in $\mathcal{W}_P [\Theta \Phi^*]$
$\Phi^* \int \Theta \Phi^* \mathcal{W}_P [\Theta \Phi^* \mathbf{d}] d\gamma'$	$N^2 Z$	$NZ$	2 for $\int \Theta \cdot d\gamma'$

vectors  $\{\mathbf{v}_i\}$ . By inserting the SVD and reorganizing to cancel indeterminacies, we obtain

$$(7) = \langle \mathcal{A}\tilde{\Phi}, \mathcal{V}\Phi \rangle = \frac{|\mathbb{U}||\mathbb{V}^*|}{N!} \sum_{j=1}^N \prod_{i \neq j} s_i \int V(\mathbf{r}) \Phi^* \mathbf{v}_j \mathbf{u}_j^* \tilde{\Phi} d\gamma \quad \text{and} \quad (196)$$

$$(8) = \langle \mathcal{A}\tilde{\Phi}, \mathcal{W}\Phi \rangle =$$

$$\frac{|\mathbb{U}||\mathbb{V}^*|}{N!} \sum_{j=1}^{N-1} \sum_{k=j+1}^N \prod_{i \neq j,k} s_i \int \Phi^* \mathbf{v}_j \mathbf{u}_j^* \tilde{\Phi} \mathcal{W}_P [\Phi^* \mathbf{v}_k \mathbf{u}_k^* \tilde{\Phi}] - \Phi^* \mathbf{v}_j \mathbf{u}_k^* \tilde{\Phi} \mathcal{W}_P [\Phi^* \mathbf{v}_k \mathbf{u}_j^* \tilde{\Phi}] d\gamma. \quad (197)$$

Similarly, the formula (17) requires application of  $\mathbb{D}^{-1}$  and multiplication by  $|\mathbb{D}|$ . Using now the SVD of  $\mathbb{D}$ , we can compute it using

$$(17) = A(l, l')(\gamma, \gamma') = \frac{|\mathbb{U}||\mathbb{V}^*|}{N!} \left( \prod_i s_i \delta(\gamma - \gamma') - \sum_{j=1}^N \prod_{i \neq j} s_i \mathbf{y}^*(\gamma) \mathbf{v}_j \mathbf{u}_j^* \mathbf{w}(\gamma') \right). \quad (198)$$

Finally, the formula (21) requires application of  $\mathbb{E}^{-1}$  and multiplication by  $|\mathbb{E}|$ . Using now the SVD of  $\mathbb{E}$ , we can compute it using

$$\begin{aligned} (21) = & \frac{|\mathbb{U}||\mathbb{V}^*|}{N!} \mathcal{F} \left[ \prod_i s_i V(\mathbf{r}) \Phi^* \mathbf{d}(\gamma) + \right. \\ & \Phi(\gamma)^* \left( \mathbf{d} \sum_{j=1}^N \prod_{i \neq j} s_i \mathcal{W}_P [\Phi^* \mathbf{v}_j \mathbf{u}_j^* \mathcal{F} \tilde{\Phi}] - \sum_{j=1}^N \mathbf{v}_j \prod_{i \neq j} s_i \mathcal{W}_P [\Phi^* \mathbf{d} \mathbf{u}_j^* \mathcal{F} \tilde{\Phi}] \right) (\gamma) \\ & + \Phi(\gamma)^* \left( \mathbf{d} \sum_{j=1}^N \prod_{i \neq j} s_i \int V(\mathbf{r}') \Phi^* \mathbf{v}_j \mathbf{u}_j^* \mathcal{F} \tilde{\Phi} d\gamma' - \sum_{j=1}^N \mathbf{v}_j \prod_{i \neq j} s_i \int V(\mathbf{r}') \Phi^* \mathbf{d} \mathbf{u}_j^* \mathcal{F} \tilde{\Phi} d\gamma' \right. \\ & + \mathbf{d} \sum_{j=1}^{N-1} \sum_{k=j+1}^N \prod_{i \neq j,k} s_i \int \Phi^* \mathbf{v}_j \mathbf{u}_j^* \mathcal{F} \tilde{\Phi} \mathcal{W}_P [\Phi^* \mathbf{v}_k \mathbf{u}_k^* \mathcal{F} \tilde{\Phi}] - \Phi^* \mathbf{v}_j \mathbf{u}_k^* \mathcal{F} \tilde{\Phi} \mathcal{W}_P [\Phi^* \mathbf{v}_k \mathbf{u}_j^* \mathcal{F} \tilde{\Phi}] d\gamma' \\ & \left. \left. - \sum_{j=1}^N \mathbf{v}_j \sum_{k=1, \neq j}^N \prod_{i \neq j,k} s_i \int \Phi^* \mathbf{d} \mathbf{u}_j^* \mathcal{F} \tilde{\Phi} \mathcal{W}_P [\Phi^* \mathbf{v}_k \mathbf{u}_k^* \mathcal{F} \tilde{\Phi}] - \Phi^* \mathbf{d} \mathbf{u}_k^* \mathcal{F} \tilde{\Phi} \mathcal{W}_P [\Phi^* \mathbf{v}_k \mathbf{u}_j^* \mathcal{F} \tilde{\Phi}] d\gamma' \right) \right]. \quad (199) \end{aligned}$$

## E. Validation tests

These tests should be run for various requested accuracies and various values of  $Z$ .

1. Construct  $\varphi$  in (125), compute  $\|\varphi\|_2$  and  $\|\varphi\|_4$ , and compare with the exact values 1 and  $2^{-3/4} \pi^{-1/4} Z^{3/4}$  from (128).
2. From  $\varphi$  compute  $\varphi^2$ , compute  $\|\varphi^2\|_1$  and  $\|\varphi^2\|_2$ , and compare with the exact values 1 and  $2^{-3/2} \pi^{-1/2} Z^{3/2}$  from (130).
3. From  $\varphi^2$ , compute  $\langle V, \varphi^2 \rangle$  and compare with the exact value  $-Z^2$  from (132).
4. From  $\varphi$  compute  $V\varphi$ , compute  $\|V\varphi\|_{4/3}$ , and compare with the exact value  $Z^{5/4} 2^{-1} 3^{5/4} \pi^{1/4} \Gamma(5/3)^{3/4}$  from (134).
5. From  $\varphi^2$  compute  $\mathcal{W}_P[\varphi^2]$ , compute  $\langle \varphi^2, \mathcal{W}_P[\varphi^2] \rangle$ , and compare with the exact value  $(5/8)Z$  from (140).

6. From  $V\varphi$ , construct the single-electron Green function  $\mathcal{G}_{-Z^2/2}$  (see Sec. II C 4), compute  $\mathcal{G}_{-Z^2/2}V\varphi$ , compute  $\|\varphi + \mathcal{G}_{-Z^2/2}V\varphi\|_2$  and  $\|\varphi + \mathcal{G}_{-Z^2/2}V\varphi\|_4$ , and compare with the exact value 0. Iterate to assure accuracy does not degrade.

Tests similar to 1 and 2 can be performed on Gaussians. Tests 3 and 5 can be attempted without using the function spaces we specified, as can a test similar to 6.

## ACKNOWLEDGMENTS

This material is based upon work supported by the National Science Foundation under Grant No. DMS-0545895.

- <sup>1</sup> G. Beylkin and M. J. Mohlenkamp, "Numerical operator calculus in higher dimensions," *Proc. Natl. Acad. Sci. U.S.A.* **99**, 10246–10251 (2002).
- <sup>2</sup> G. Beylkin and M. J. Mohlenkamp, "Algorithms for numerical analysis in high dimensions," *SIAM J. Sci. Comput.* **26**, 2133–2159 (2005).
- <sup>3</sup> G. Beylkin, M. J. Mohlenkamp, and F. Pérez, "Approximating a wavefunction as an unconstrained sum of Slater determinants," *J. Math. Phys.* **49**, 032107 (2008).
- <sup>4</sup> M. J. Mohlenkamp, "A center-of-mass principle for the multiparticle Schrödinger equation," *J. Math. Phys.* **51**, 022112–1–022112–15 (2010).
- <sup>5</sup> M. J. Mohlenkamp, "Capturing the Interelectron Cusp Using a Geminal Layer on an Unconstrained Sum of Slater Determinants," *SIAM J. Appl. Math.* **72**, 1742–1771 (2012).
- <sup>6</sup> R. J. Harrison, G. I. Fann, T. Yanai, and G. Beylkin, "Multiresolution quantum chemistry in multiwavelet bases," in *Lecture Notes in Computer Science. Computational Science-ICCS 2003*, edited by P. M. A. Sloot *et al.* (Springer, 2003), Vol. 2660, pp. 103–110.
- <sup>7</sup> R. J. Harrison, G. I. Fann, T. Yanai, Z. Gan, and G. Beylkin, "Multiresolution quantum chemistry: Basic theory and initial applications," *J. Chem. Phys.* **121**, 11587–11598 (2004).
- <sup>8</sup> G. Beylkin, V. Cheruvu, and F. Pérez, "Fast adaptive algorithms in the non-standard form for multidimensional problems," *Appl. Comput. Harmon. Anal.* **24**, 354–377 (2008).
- <sup>9</sup> A. Uschmajew, "Regularity of tensor product approximations to square integrable functions," *Constructive Approx.* **34**, 371–391 (2011).
- <sup>10</sup> G. B. Folland, *Real Analysis: Modern Techniques and their Applications*, 2nd ed., Pure and Applied Mathematics (John Wiley & Sons Inc., New York, 1999), pp. xvi+386.
- <sup>11</sup> E. Stein and G. Weiss, *Fourier Analysis on Euclidean Spaces* (Princeton University Press, Princeton, NJ, 1971).
- <sup>12</sup> See <http://dlmf.nist.gov/> for NIST Digital Library of Mathematical Release 1.0.5 of 2012-10-01, online companion to Ref. 17.
- <sup>13</sup> G. Beylkin and L. Monzón, "Approximation by exponential sums revisited," *Appl. Comput. Harmon. Anal.* **28**, 131–149 (2010).
- <sup>14</sup> L. Saloff-Coste, *Aspects of Sobolev-Type Inequalities*, London Mathematical Society Lecture Note Series Vol. 289 (Cambridge University Press, Cambridge, 2002), pp. x+190.
- <sup>15</sup> H. Yserentant, *Regularity and Approximability of Electronic Wave Functions*, Lecture Notes in Mathematics Vol. 2000 (Springer-Verlag, Berlin, 2010), pp. viii+182.
- <sup>16</sup> G. Golub and C. Van Loan, *Matrix Computations*, 3rd ed. (Johns Hopkins University Press, 1996).
- <sup>17</sup> *NIST Handbook of Mathematical Functions*, edited by F. W. J. Olver, D. W. Lozier, R. F. Boisvert, and C. W. Clark (Cambridge University Press, New York, NY, 2010), print companion to Ref. 12.